

## Corticotropin-Releasing Hormone Receptor Antagonists: Framework Design and Synthesis Guided by Ligand Conformational Studies

C. Nicholas Hodge,\* Paul E. Aldrich, Zelda R. Wasserman, Christina H. Fernandez, Gregory A. Nemeth, Argyrios Arvanitis, Robert S. Cheeseman, Robert J. Chorvat, Engelbert Ciganek, Thomas E. Christos, Paul J. Gilligan, Paul Krenitsky,<sup>†</sup> Everett Scholfield, and Philip Strucely<sup>‡</sup>

Department of Chemical and Physical Sciences, DuPont Pharmaceuticals Company, Experimental Station, P.O. Box 80500, Wilmington, Delaware 19880-0500

Received October 1, 1998

As described in the preceding paper (Arvanitis et al. *J. Med. Chem.* 1999, 42), anilino-pyrimidines **I** were identified as potent antagonists of corticotropin-releasing hormone-1 receptor (CRH<sub>1</sub>-R, also referred to as corticotropin-releasing factor, CRF<sub>1</sub>-R). Our next goal was to understand the receptor-bound conformation of the antagonists and to use this information to help guide preclinical optimization of the series and to develop new leads. Since receptor structural information was not available, we assumed that these small, high-affinity antagonists would tend to bind in conformations at or energetically close to their global minima and that rigid analogues that maintained the important stereoelectronic features of the bound anilino-pyrimidine would also bind tightly. Conformational preferences and barriers to rotation of the anilino-pyrimidines were determined by semiempirical methods, and X-ray and variable-temperature NMR spectroscopy provided experimental results that correlated well with calculated structures. Using these data, a key dihedral angle was constrained to design fused-ring analogues, substituted *N*-arylpyrrolopyridines **II**, synthesis of which provided CRH<sub>1</sub> receptor antagonists with potency equal to that of the initial congeneric leads ( $K_i = 1$  nM) and which closely matched the conformation held by the original compound, as determined by crystallography. In addition to providing a useful template for further analogue synthesis, the study unequivocally determined the active conformation of the anilino-pyrimidines. Theoretical and spectroscopic studies, synthesis, and receptor binding data are presented.

### Introduction

As described in the first paper in this series,<sup>1</sup> there is strong evidence that potent, bioavailable antagonists of the corticotropin-releasing hormone (CRH<sub>1</sub>) receptor (CRH<sub>1</sub>-R) will have clinically beneficial properties in a number of indications, particularly anxiety and depression. Having discovered potent anilino-pyrimidine antagonists **I** (Chart 1), the next task was to broaden the scope of the lead into new structural classes. For the project to be considered successful, we determined that new antagonists should have: (1) potency equal to or greater than that of the original lead; (2) a novel core structure that would provide insight into the bound conformation and allow us to rapidly and systematically explore the effect of changes in side chain functionality; (3) a favorable oral bioavailability potential (that is, the size, functional groups, and polarity of potent compounds in the new series should be within the ranges associated with favorable absorption, distribution, metabolism, and elimination profiles<sup>2</sup>); (4) a favorable potential for distribution into the CNS;<sup>3</sup> (5) a stable, formulatable, nontoxic core structure.

Achieving this goal would provide several advantages to our program: first, it would expand our knowledge of active structures in addition to the anilino-pyrimidine

series. Additionally, whether the new series was ultimately as attractive as the anilino-pyrimidines in one or more of the above areas, the process of design, if carefully executed, would provide insight into the bound shape of the original lead and thereby assist in optimization of the anilino-pyrimidines. Finally, different core structures would broaden the scope of functionality that could be introduced into the molecules, by virtue of different chemistry.

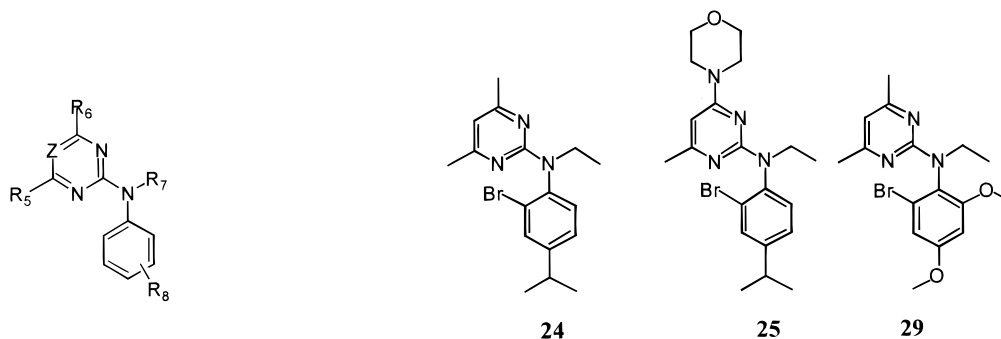
In designing the new structural series, we were guided by an active ligand rather than its receptor. The CRH<sub>1</sub> receptor is a seven-helical bundle that spans the cell membrane, and although its tertiary structure is qualitatively well-understood, it was clear that current receptor models possessed insufficient accuracy for design at the atomic level. Additionally, unlike the catecholamine neurotransmitter receptors, which are known to interact with a critical aspartic acid on transmembrane helix 3, significant uncertainty existed even as to *where* ligands bind the receptor, i.e., inside or outside the seven-helix bundle, inserted into the membrane, or extra- or even intracellularly.<sup>4</sup> Kinetic data suggested that unlike peptide CRH-based antagonists,<sup>5</sup> the anilino-pyrimidines do not compete with peptide agonists (S. Culp, unpublished results) in receptor-binding assays, which obviated the use of models of the bound natural agonist for mimicking the effect of anilino-pyrimidines.

The most direct and reliable method for new ligand design was therefore to understand the bound shape of

\* Corresponding author. Current address: Caliper Technologies Corp., 605 Fairchild Dr., Mountain View, CA 94043-2234. E-mail: nick.hodge@calipertech.com.

<sup>†</sup> Current address: ArQule, Inc., 200 Boston Ave, Medford, MA 02155.

<sup>‡</sup> Deceased.

**Chart 1.** Optimum Anilinopyrimidine Substituents for CRH<sub>1</sub>-R Potency

<b>Z:</b>	CH, N	e.g.	<b>24:</b> rCRH <sub>1</sub> R Ki = 46 nM
<b>R<sub>5</sub>:</b>	methyl		<b>25:</b> rCRH <sub>1</sub> R Ki = 22 nM
<b>R<sub>6</sub>:</b>	small to large lipophilic, neutral or weakly basic groups		<b>29:</b> rCRH <sub>1</sub> R Ki = 5 nM
<b>R<sub>7</sub>:</b>	small (C1-C3) alkyl or alkenyl groups		
<b>R<sub>8</sub>:</b>	2-position: medium-sized lipophilic groups (halogen, -SMe)		
	4-position, medium-sized lipophilic groups or weak H-bond acceptors		
	6-position: small to medium-sized lipophilic groups (H, -OMe, -SMe).		

the already-identified lead series and to design molecules that present these features rigidly and unambiguously in space. This process is conceptually similar to other successful structure-based designs;<sup>6,7</sup> here our emphasis is on the rigorous determination of the bound ligand conformation using information derived only from free ligand spectra and calculations.

The method we employed to design the new series involved the following steps: (1) Determine low-energy conformations of potent anilinopyrimidines by NMR, X-ray, and semiempirical methods. (2) Design conformationally restricted analogues, starting with the most favorable conformation. (3) Synthesize the compounds and characterize their three-dimensional shape. (4) Test for biological activity, and if necessary redesign based on the next-lowest-lying conformation.

This approach depends on the hypothesis that a low-energy free conformation is predictive of the bound conformation. Explicitly stating this assumption highlights the importance of examining low-energy conformations under several conditions: in crystals, in non-polar and polar solvents, and calculated in the gas phase. Clearly this assumption will not always hold. However, in the absence of a known bound geometry for these molecules, the lowest energy is a good place to start. These are small, potent molecules, and only limited interactions are available for binding to the receptor. It is reasonable to suggest, therefore, that in order to avoid an internal strain energy penalty on binding, the internal strain energy of the bound conformation will be close to the lowest energy conformation available in the test medium (in this case pH 7.2 buffer). This hypothesis obviously does not imply that the bound conformer and the low-energy free conformer are *geometrically* close, so a careful analysis requires examination of the full potential energy surface of the molecule in question. It is also possible that a high-energy ligand conformation is stabilized by a high-energy receptor conformation, and the resulting complex

is lower in energy than the two free species. This occurrence is uncommon with small ligands, in our experience. In any case, if the conformational locking is done carefully, a negative result is also valuable since it rules out one of a few possible bound conformations. It should also be clear that this approach becomes experimentally untenable as the number of equi-energetic minima occupied by the reference ligand increases. The use of structural and computational chemistry to obtain a detailed understanding of the conformational free energy surface of the reference ligand is therefore a useful initial step in deciding whether this approach is appropriate.

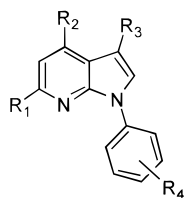
In this report we detail the successful application of this method to the design, synthesis, and characterization of CRH<sub>1</sub>-R antagonists (Table 1) that meet the criteria described above. The anilinopyrimidines that were characterized spectrally and computationally were synthesized as described in the first paper in this series and are summarized in Table 2. A limited structure-activity study of these potent bicyclic antagonists is presented here as well. The third paper in this series<sup>8</sup> reports expanded SAR studies on bicyclic analogues, as well as a summary of reports on related antagonists from other laboratories.

## Methods

**Single-Crystal X-ray Analysis.** Structural characterization of compounds **2**, **3**, **9**, **25**, and **29** (Tables 1 and 2) was carried out using standard X-ray crystallographic techniques. Complete reports including crystallization conditions, atomic coordinates, thermal parameters, and interatomic distances and angles are available as Supporting Information.

**NMR Solution Structure.** Variable-temperature <sup>1</sup>H NMR experiments were carried out on a Varian XL-400 spectrometer at 5–10 mg of sample/mL of solvent.

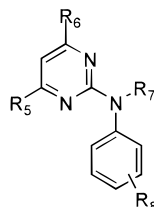
Table 1.



no.	R <sub>1</sub>	R <sub>2</sub>	R <sub>3</sub>	R <sub>4</sub>	yield <sup>a</sup> (%)	mp (°C)	anal.	X-ray <sup>g</sup>	K <sub>i</sub> (nM)
1	Me	Me	CN	2-Br, 4-isopropyl	78	108	C,H,N		363
2	Me	Me	H	2-Br, 4-isopropyl	66	76	C,H,N	✓	47
3	Ph	Me	CN	2-Br, 4-isopropyl	77	130	C,H,N	✓	>10 <sup>4</sup>
4	Me	Ph	CN	2-Br, 4-isopropyl	2 <sup>b</sup>	198	C,H,N		34
5	Me	Ph	H	2-Br, 4-isopropyl	92	115	C,H,N		36
6	Ph	Me	H	2-Br, 4-isopropyl	82	96	C,H,N		>10 <sup>4</sup>
7	Me	Me	CN	2-Br, 4,6-(OMe) <sub>2</sub>	92	186	C,H,N		29
8	Me	Me	H	2-Br, 4,6-(OMe) <sub>2</sub>	20 <sup>c</sup>	202	C,H,N		1
9	Me	H	CN	2-Br, 4-isopropyl	10	125	C,H,N	✓	1277
10	H	Me	CN	2-Br, 4-isopropyl	10 <sup>d</sup>	176	C,H,N		>10 <sup>4</sup>
11	Me	H	H	2-Br, 4-isopropyl	57	oil	C,H,N		222
12	H	Me	H	2-Br, 4-isopropyl	85	oil	C,H,N		>10 <sup>4</sup>
13	OH <sup>e</sup>	Me	CN	2-Br, 4-isopropyl	45	202	HRMS		>10 <sup>4</sup>
14	Cl	Me	CN	2-Br, 4-isopropyl	56	124	C,H,N <sup>f</sup>		446
15	Cl	Me	H	2-Br, 4-isopropyl	79	75	C,H,N		79
16	Me	H	CN	2-Br, 4-isopropyl (7-N-oxide)	71	179	C,H,N		>10 <sup>4</sup>
17	Me	Cl	CN	2-Br, 4-isopropyl	41	123	C,H,N		722
18	Me	Cl	H	2-Br, 4-isopropyl	73	oil	C,H,N		67
19	Me	1-morpholino	CN	2-Br, 4-isopropyl	62	192	C,H,N		112
20	Me	1-morpholino	H	2-Br, 4-isopropyl	73	101	C,H,N		28
21	Me	Me	H	4-isopropyl	100	oil	C,H,N		2462
22	Me	Me	CONH <sub>2</sub>	2-Br, 4-isopropyl	89	237	HRMS		>10 <sup>4</sup>
23	Me	Me	CO <sub>2</sub> H	2-Br, 4-isopropyl	65	242	HRMS		>10 <sup>4</sup>

<sup>a</sup> Last step. <sup>b</sup> Side product from preparation of **4**. <sup>c</sup> Yields suffered from O-demethylation; cited yield is after remethylation. See Experimental Section. <sup>d</sup> Coproduct from preparation of **9**; total yield of **9** + **10** was 21%. <sup>e</sup> Or keto tautomer. <sup>f</sup> Microanalysis not accurate—see Experimental Section. <sup>g</sup> Check (✓) indicates these data were obtained and appear in the Supporting Information.

Table 2.



no.	R <sub>5</sub>	R <sub>6</sub>	R <sub>7</sub>	R <sub>8</sub>	T <sub>c1</sub> (°C) <sup>a</sup>	ΔG <sub>act-1</sub> (kcal) <sup>a</sup>	T <sub>c2</sub> (°C) <sup>b</sup>	ΔG <sub>act-2</sub> (kcal) <sup>b</sup>	X-ray <sup>c</sup>	K <sub>i</sub> (nM)
24	Me	Me	Et	2-Br, 4-isopropyl						46
25	Me	morpholino	Et	2-Br, 4-isopropyl					✓	22
26	Me	Me	Me	2-Br, 4-isopropyl						96
27	Me	Me	Me	2-I, 4-isopropyl	0	13.9	<-70	[<9] <sup>f</sup>		48
28	Me	Me	Et	2-I, 4-isopropyl	0	14.7	90	17.7		38
29	Me	Me	Et	2,4-dimethoxy, 6-Br	100	20.3	>150		✓	5
30	Me	Cl	Et	2-I, 4-isopropyl	20	16.9	120	19.2		<i>d</i>
31					140	22.5	>150			43 <sup>e</sup>
32					>150	[>23] <sup>f</sup>	100	18.2		>1000

<sup>a</sup> Coalescence temperature and calculated activation energy for pyrimidine methyl group(s). <sup>b</sup> Coalescence temperature and calculated activation energy for N-CH<sub>2</sub> group, where applicable. <sup>c</sup> Check (✓) indicates these data were obtained and appear in the Supporting Information. <sup>d</sup> K<sub>i</sub> values of chloropyrimidines were not considered reliable due to potential reactivity under assay conditions. The potency is approximately equal to that of the dimethylpyrimidine. <sup>e</sup> Methanesulfonate salt. <sup>f</sup> Assumes the same Δν value as **28**. Compounds listed in this table were synthesized as described in the first paper in this series.<sup>1</sup>

Acquisition and delay times were 4.07 and 2 s, respectively, and pulse width was 4.62 μs. Normally 32 transients were collected at each temperature. Data

were collected at 20–40 °C increments, from –70 to 30 °C (CD<sub>2</sub>Cl<sub>2</sub>), –50 to 30 °C (CDCl<sub>3</sub>), or 30 to 150 °C (DMSO-*d*<sub>6</sub>).

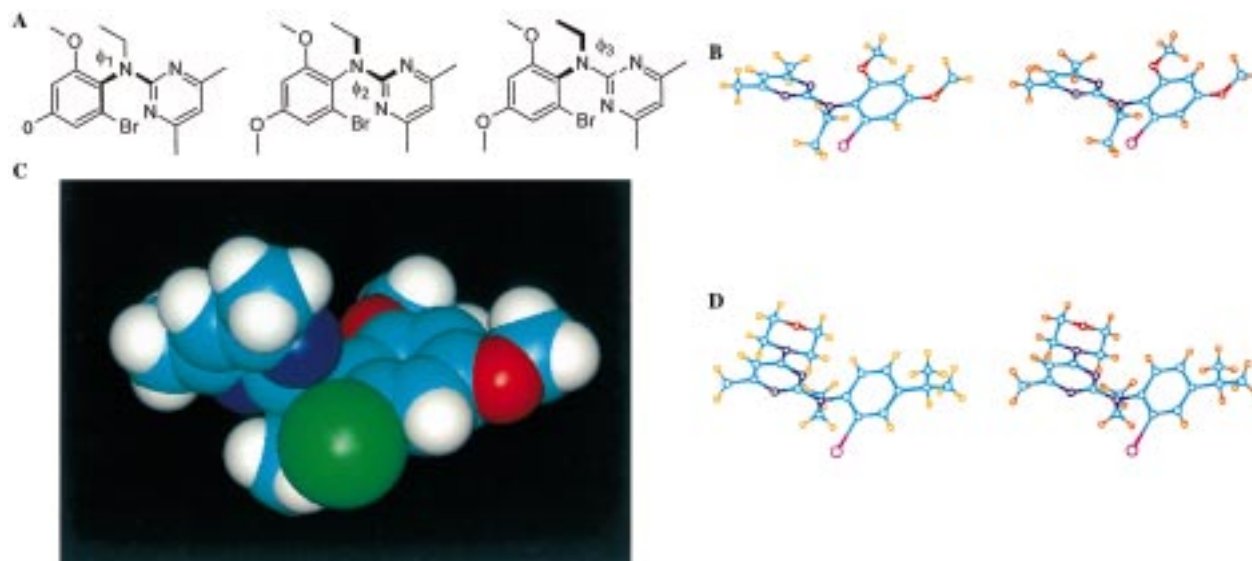


**Figure 1.** A. Key dihedrals in X-ray structure of **29**:  $\phi_1 = 108^\circ$ ,  $\phi_2 = 4^\circ$ ,  $\phi_3 = 169^\circ$ . B. Stereoview of X-ray structure of **29**. C. Space-filling model of X-ray structure of **29**. D. Stereoview of X-ray structure of **25**.

**Conformational Analysis.** For reasons presented in the Results and Discussion section, preliminary modeling indicated that molecular mechanics force fields would not provide accurate low-energy conformations of the anilino-pyrimidines. As a result, exploration of the potential surface and calculation of rotational barriers were done with the program MOPAC using the AM1 Hamiltonian.<sup>9,10</sup>

To calculate the potential surface, an initial model of compound **29** was built and minimized in Discover using the cff91 force field.<sup>11</sup> Starting with this geometry, the key dihedrals ( $\phi_1$  and  $\phi_2$ , Figure 1A) were rotated in  $30^\circ$  increments, and each of the 144 single-point energies was determined in MOPAC. Minima were located, and each of them was fully minimized.

To calculate the barrier to rotation about selected bonds, we started from the global minimum and changed the dihedral angle by  $20^\circ$  increments. Smaller ( $4^\circ$ ) increments were used near the transition maxima. This dihedral was held fixed, and the structure was minimized in MOPAC. The force-constant matrix was diagonalized to verify that these were transition states.

**Chemistry.** The target antagonists, as discussed below, contained the 1-phenyl-7-azaindole or 1*H*-pyrrolo[2,3-*b*]pyridine core (Table 1; hereafter referred to as pyrrolopyridines). The chemistry of pyrrolopyridines has been studied in some depth by Yakhontov<sup>12</sup> and was reviewed by Willette.<sup>13</sup> Derivatives with different substitution patterns than those described here have been reported as CNS depressants and antihypertensives.<sup>14</sup> Brodrick and Wibberley<sup>15</sup> described a synthesis that provided entry into a substitution pattern that was ideal for our purposes (Scheme 1). The syntheses of cyanopyrrolopyridines **1**, **3**, **7**, **9**, **10**, and **13** (Table 1) were carried out following the basic procedure published by these authors, with modifications described in the Experimental Section. In this reference the authors assign the major cyclization product of *N*-phenylpyrrole **IV** (Scheme 1) with 1-phenylbutane-1,3-dione as the 6-methyl-4-phenylpyrrolopyridine isomer, based on NMR shifts in analogous compounds. In our hands, with an

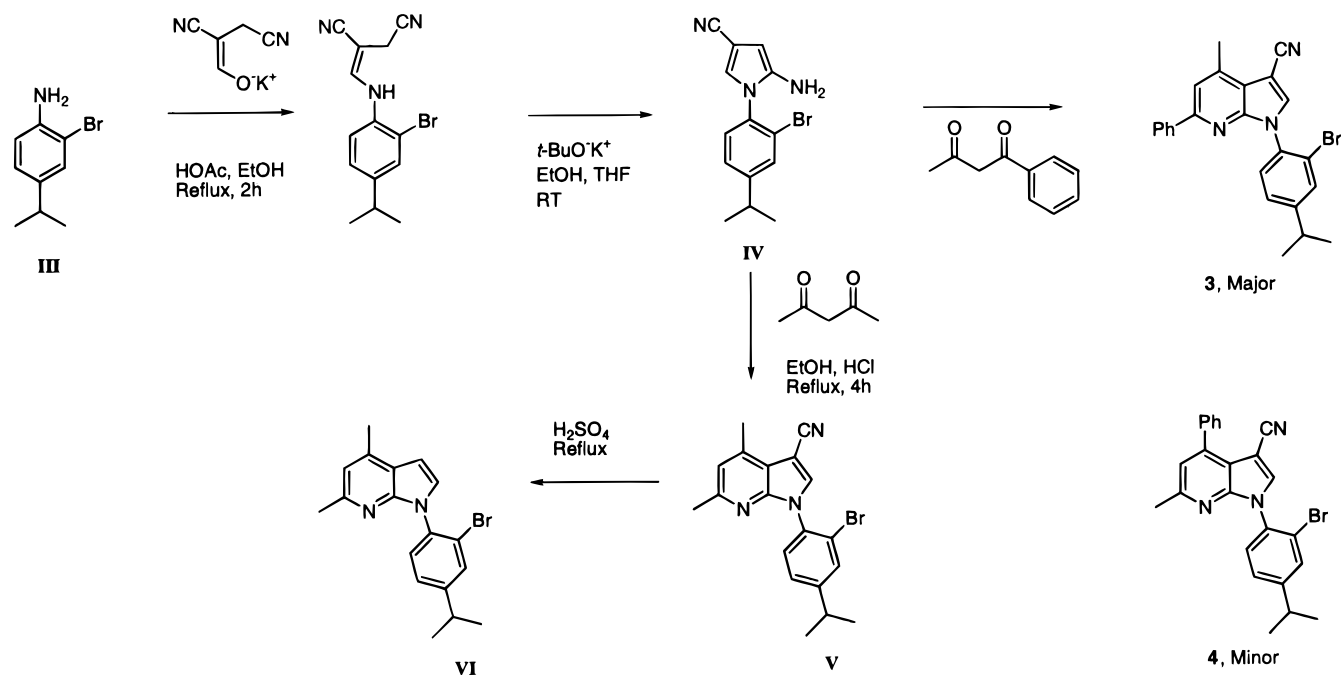
ortho-substituted phenyl ring but under similar conditions (ethanol/concentrated HCl at reflux), the 4-methyl-6-phenyl isomer **3** is in fact the dominant product, as shown by X-ray crystallography (see Supporting Information). The 4-phenyl isomer could be isolated in very small amounts from this reaction mixture. Alternatively, the yield of **4** could be improved at the expense of overall yield by running the reaction under conditions that favored initial attack by nitrogen onto the less hindered carbonyl (refluxing xylene with removal of water; see Experimental Section). The 3-carboxamido- and 3-carboxypyrrolopyrimidines **22** and **23** (Table 1) were also prepared by procedures described in this reference.

The 3-unsubstituted derivatives, **2**, **5**, **6**, **8**, **11**, and **12** were prepared in a single step by treatment of the appropriate nitrile with 65% sulfuric acid at reflux (approximately  $140^\circ\text{C}$ ) for 1 h. The ring system is remarkably stable to this treatment; yields are summarized in Table 1.

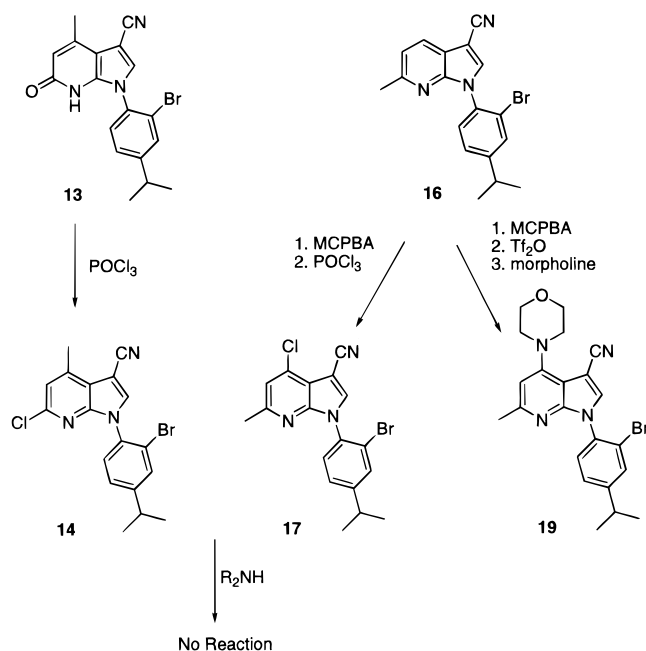
The 4- and 6-chloro derivatives **14**, **15**, **17**, and **18** (Table 1 and Scheme 2) were examined as intermediates for the exploration of non-carbon-linked substituents at these positions. The 6-chloro derivative **14** was prepared from pyridone **13** in low yield, and elemental analyses were poor. However, the cyano group was removed without difficulty to form **15**, which was characterized adequately. The 4-chloro derivative was prepared via oxidation of the pyridyl nitrogen of 4-unsubstituted derivative **9** to *N*-oxide **16**, followed by displacement in the 4-position with phosphorus oxychloride. (Mixtures of products were reported under similar Meisenheimer conditions on naphthyridine *N*-oxide,<sup>16</sup> but since the 6-position was blocked in our case, the reaction went smoothly.) Unfortunately, displacing chloride failed under all conditions attempted. Under forcing conditions, reaction with the aryl bromide occurred. After considerable experimentation the *N*-oxide was treated with triflic anhydride followed directly by morpholine,



## Scheme 1



## Scheme 2



forming **19** in moderate yields. The nitrile was removed under standard conditions to form 4-morpholino derivative **20**.

The anilino-pyrimidine antagonists shown in Table 2 were synthesized as described in the first paper in this series.<sup>1</sup> During the course of this work,<sup>17,18</sup> the group at Pfizer disclosed the CRH affinity of related bicyclic systems.<sup>19</sup> The full scope of the chemistry of the bicyclic antagonists is discussed in more detail in the following paper in this series.<sup>8</sup>

## Results and Discussion

**X-ray Structure Analysis.** As a starting point for analyzing the low-energy conformations of anilino-pyrimidines, a single-crystal X-ray structure of compound

**29** was obtained, shown as a stereo ball-and-stick model in Figure 1B. The important geometric features for designing a conformationally locked mimetic are the following: the phenyl and pyrimidine rings form a plane angle of  $56^\circ$ , the central nitrogen has a pronounced pucker of  $17^\circ$ , and the N-C-N-C dihedral angle,  $\phi_2$ , between the pyrimidine ring and the central nitrogen, is almost planar, at  $4^\circ$ .

A space-filling model (Figure 1C) clearly shows the steric hindrance around the two bonds joining the central nitrogen. Only one molecule lies in the unit cell, and intermolecular contacts do not appear to contribute to the observed geometry (see Supporting Information). Note there are no H-bond donor-acceptor pairs available in the molecule, and no solvent appears in the unit cell.

A crystal structure of asymmetrically substituted pyrimidine **25** was also obtained (Figure 1D). Here the plane angle between phenyl and pyrimidine rings is  $84^\circ$ , the pucker angle of the anilino nitrogen is only  $5^\circ$ , and the N-C-N-C dihedral,  $\phi_2$ , is also  $4^\circ$ . Interestingly, the rotamer which places the morpholino group close to the phenyl ring is observed in the crystalline state. In the following discussions, the pyrimidine substituent that lies closest to the phenyl ring (e.g., the morpholino group in the case of **25**) is referred to as the endo group, and the more distant group is referred to as exo. The same nomenclature is used for the pyrimidine ring nitrogens.

**NMR Solution Structure.** Since the crystal environment may not accurately represent conformational minima in solution, and to obtain an understanding of the dynamic conformational behavior of these molecules, we examined variable-temperature  $^1\text{H}$  NMR spectra. It seemed likely that the steric hindrance observed in the X-ray structure around the anilino nitrogen would result in discrete observable conformations at experimentally accessible temperatures. Spectra were recorded (see Methods section) at various increments from  $-70$  to  $30$

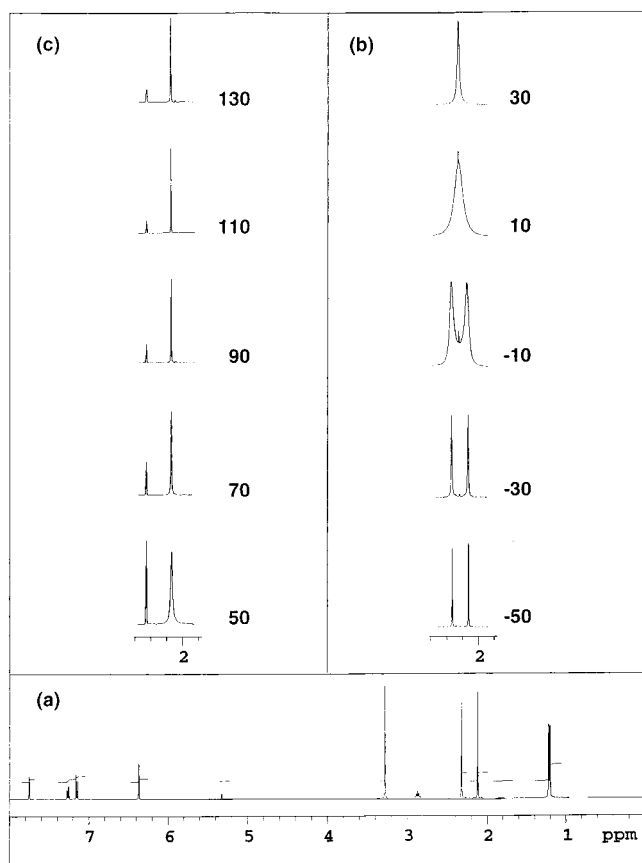
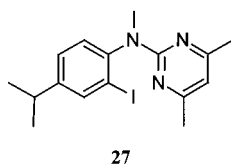


**Figure 2.** Variable-temperature NMR of **27**. a. Spectrum at  $-70\text{ }^{\circ}\text{C}$  in  $\text{CD}_2\text{Cl}_2$ . b. Spectra at indicated temperatures in  $\text{CD}_2\text{Cl}_2$ , showing pyrimidine methyl resonances. c. Spectra at indicated temperatures in  $\text{DMSO}-d_6$ , showing pyrimidine methyl resonances. Peak height is normalized such that highest peak is full scale.

$^{\circ}\text{C}$  ( $\text{CD}_2\text{Cl}_2$ ) and from  $30$  to  $150\text{ }^{\circ}\text{C}$  ( $\text{DMSO}-d_6$ ). A representative experiment with 2-(*N*-methyl-*N*-(2-iodo-4-isopropylphenyl)amino)-4,6-dimethylpyrimidine (**27**) is shown in Figure 2. The pyrimidine methyl groups at  $2.1$  and  $2.3$  ppm are in distinct chemical environments at  $-70\text{ }^{\circ}\text{C}$  in  $\text{CD}_2\text{Cl}_2$  (Figure 2a), with reasonably small line widths. By  $-30\text{ }^{\circ}\text{C}$ , noticeable broadening has occurred, and the peaks coalesce somewhere between  $-10$  and  $10\text{ }^{\circ}\text{C}$  (Figure 2b). When  $\text{DMSO}-d_6$  is solvent (Figure 2c), the peak is still broad at  $30\text{ }^{\circ}\text{C}$  but sharpens to a minimum width by  $90\text{ }^{\circ}\text{C}$ , indicating free rotational averaging of the methyl groups. The *N*-methyl hydrogens are equivalent even at the lowest temperature ( $-70\text{ }^{\circ}\text{C}$ ).

Spectra of the *N*-ethyl analogue **28** under the same conditions are shown in Figure 3. The coalescence temperature ( $T_{c1}$ ) of the pyrimidine methyls remains the same ( $\sim 0\text{ }^{\circ}\text{C}$ ). The behavior of the two methylene protons next to the central nitrogen is informative in this compound. The protons are well-separated at low temperature (dt,  $3.35$  ppm; dt,  $4.25$  ppm; Figure 3a). Some broadening is visible at  $30\text{ }^{\circ}\text{C}$  in  $\text{CD}_2\text{Cl}_2$  (Figure

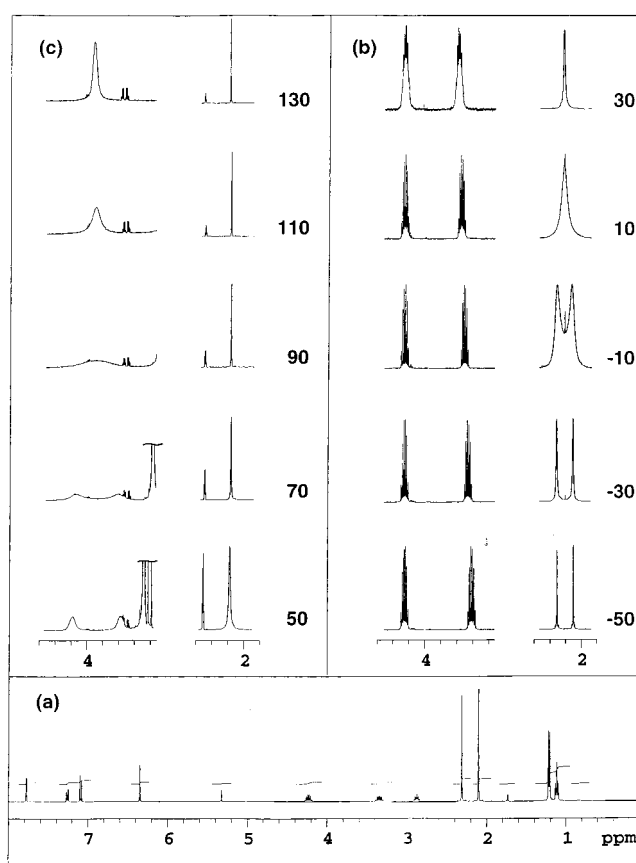
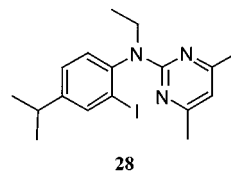


**Figure 3.** Variable-temperature NMR of **28**. a. Spectrum at  $-70\text{ }^{\circ}\text{C}$  in  $\text{CD}_2\text{Cl}_2$ . b. Spectra at indicated temperatures in  $\text{CD}_2\text{Cl}_2$ , showing pyrimidine methyl and *N*- $\text{CH}_2$  resonances. c. Spectra at indicated temperatures in  $\text{DMSO}-d_6$ , showing pyrimidine methyl and *N*- $\text{CH}_2$  resonances. Peak height is normalized such that highest peak is full scale.

3b), and the coalescence temperature ( $T_{c2}$ ) in  $\text{DMSO}-d_6$  is about  $90\text{ }^{\circ}\text{C}$  (Figure 3c). The peak has not fully sharpened by  $140\text{ }^{\circ}\text{C}$ , suggesting some hindered rotation even at this temperature. Over this entire range, the unhindered isopropyl methyl and methylene resonances show virtually no change in chemical shift or coupling constants.

Spectra of **29–32** were obtained similarly. Compounds **30** and **31** were particularly useful for analyzing the relative distribution and  $T_c$  of rotamers of asymmetrically substituted pyrimidines. Compound **30**, a 4-chloro-6-methylpyrimidine, shows two pyrimidine methyl peaks at low temperature, which we assign to the *exo* (downfield,  $2.17$  ppm,  $60\%$ ) and *endo* (upfield,  $2.07$  ppm,  $40\%$ ) rotamers. These peaks coalesce at about  $20\text{ }^{\circ}\text{C}$  and form a single sharp peak above  $90\text{ }^{\circ}\text{C}$ . Asymmetric 4-morpholino-6-methyltriazine **31**, on the other hand, also shows two methyl peaks but with the reverse distribution (upfield,  $1.99$  ppm,  $65\%$ , and downfield,  $2.17$  ppm,  $35\%$ ). The peaks begin to broaden at  $70\text{ }^{\circ}\text{C}$  and have not fully coalesced by  $130\text{ }^{\circ}\text{C}$ . The increase in  $T_c$  values for the 2-chloro-4-methylpyrimidine derivative

**30** and the aminotriazine **31** (Table 2) relative to the dimethylpyrimidine congeners may indicate electronic effects on the rotational barrier. Other intriguing observations were made, and some studies on the chirality of these diastereotopic molecules were carried out but were not directly relevant to the design process and will be reported elsewhere.

For the purpose of this qualitative analysis, the coalescence temperature is reported as the temperature at which coalescence is actually observed; that is, a very low, broad baseline hump is observed, as in Figure 3c (90 °C), or  $T_c$  is estimated by extrapolating between the two measurements at which it occurred, as in Figure 3b between -10 and 10 °C. The uncertainty is therefore about 5 °C; this corresponds to an error of about 0.3 kcal in the free energy of activation,  $\Delta G_{act}$ , as calculated from the Eyring equation.<sup>20</sup> The values for coalescence of the pyrimidine methyl(s) ( $T_{c1}$  and  $\Delta G_{act-1}$ ) and for coalescence of the methylene group on nitrogen ( $T_{c2}$  and  $\Delta G_{act-2}$ ), when observed, are listed in Table 2.

It has been reported<sup>21</sup> that alkoxydiarylboronates with substituents at the aryl ortho positions show similar temperature-dependent rotational averaging of protons on both the aryl and alkoxy groups, with values of  $\Delta G_{act}$  about 4–6 kcal lower than we observe in the anilinopyrimidines.

To determine if a protic environment would change the preferred low-energy conformations in solution, D<sub>2</sub>O (up to 40%, 0.8 mg/mL sample in DMSO-*d*<sub>6</sub>) was added to the NMR solvent. No significant change in the room-temperature shift positions or coupling constants of compound **27** or **28** was observed under these conditions.

An NOE between the pyrimidine methyl group and ortho ring proton of compound **28** was observed (not shown). The pyrimidine methyls are nonequivalent at room temperature, as discussed above, and the upfield-shifted methyl shows the NOE. No NOE is observed between an N-CH<sub>3</sub> proton and the ortho proton. The only conformation that is consistent with these data is one similar to the X-ray structure, in which one pyrimidine methyl is tucked in close proximity to the shielding cone of the aromatic ring. In a model of **28** based on the low-energy conformations calculated below, the distance between the centroid of the three methyl protons and the ortho aromatic proton is 4.5 Å, consistent with the observed NOE.

The need for caution in applying X-ray conformations to ligand design is underscored by the observation that unsymmetrically substituted triazine derivative **31** has both triazine rotamers present in solution under the NMR conditions, whereas the crystal structure of **25**, containing an analogously substituted pyrimidine, shows only the rotamer with the morpholine group endo to the phenyl ring (vide supra). There are a number of possible reasons for this difference: the *endo*-morpholine could have crystallized preferentially; the lowest energy conformations could differ in the crystal versus solution state; and/or the pyrimidine and triazine could have different low-energy conformations. But since the SAR of the designed pyrrolopyridine series (see below and next paper in this series<sup>8</sup>) demonstrates unequivocally that a large pyrimidine/triazine substituent is *only* tolerated at the exo position, the relevant point is that the crystal structure of **25** predicted an inactive con-

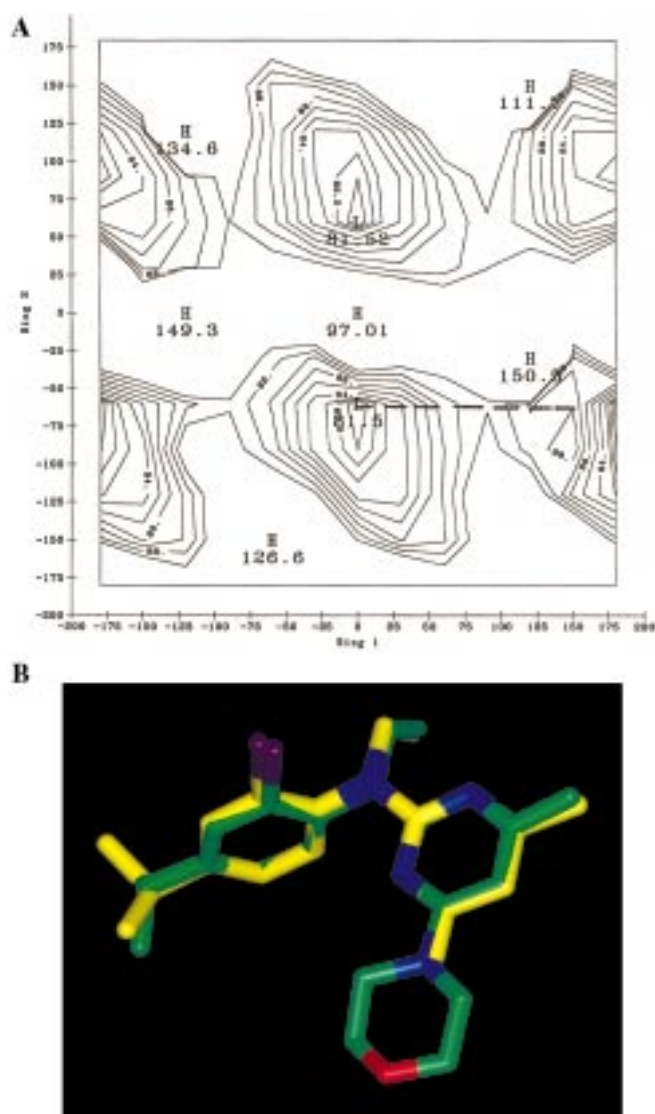


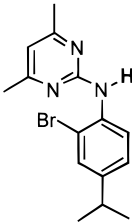
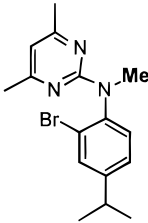
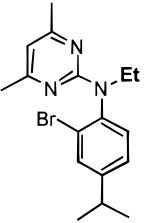
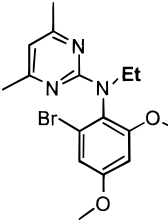
**Figure 4.** A. Contour plot of the calculated energy (1 kcal/contour line) versus dihedrals  $\phi_1$  and  $\phi_2$  of *N*-methylanilinopyrimidine **27**. The dashed lines show the lowest energy path for rotation of the pyrimidine ring to a symmetry-equivalent structure. B. Conformation of **27** (yellow carbons) at the minimum energy values of  $\phi_1$  and  $\phi_2$  overlaid with the X-ray structure of **25** (green carbons) for comparison.

formation, and the use of several methods to determine other close-lying minima is important for design.

From these experimental conformational studies it appears that a single, fairly deep-welled minimum energy structure dominates at room temperature in a variety of solvents, with values of  $\phi_{1-3}$  close to those observed in the X-ray structure. (For nonsymmetrically substituted heterocycles, two nondegenerate conformations are present.) We also now possessed experimentally determined values of  $\Delta G_{act}$  that could be used to assess the accuracy of calculated conformations.

**Calculated Low-Energy Conformations.** In addition to the insights we were obtaining into the experimentally preferred low-energy geometry of anilinopyrimidines, we also wanted to be sure that we could model these compounds accurately for purposes of design, and we wanted to determine if there were other low-lying minima not detected by spectral techniques but that might represent the receptor-bound conforma-

**Chart 2.** Effect of *N*- and 6-Phenyl Substituents on Affinity

				
rCRH <sub>1</sub> R K <sub>i</sub> , nM*:	>10,000	96	46	5
Compound #	33	27	24	29

\* See reference 1.

tion. We initially conceived a molecular field analysis<sup>22</sup> as a rapid means of understanding the bound shape of the anilino pyrimidines. We found, however, that the experimentally observed structures were not well reproduced by force fields available at the time, since the ones we examined forced the anilino nitrogen into planarity even at the expense of steric strain, which was counter to intuition and the experimental details we were accumulating. Since the limited degrees of internal freedom in the leads allowed us to undertake conformational analysis by semiempirical methods at reasonable computational cost, we performed a full analysis using MOPAC with the AM1 Hamiltonian<sup>9,10</sup> (see Methods section).

A contour plot of the calculated energy (1 kcal/contour line) versus dihedrals  $\phi_1$  and  $\phi_2$  is shown in Figure 4A for *N*-methylanilino pyrimidine **27**. The conformation at the minimum energy values of  $\phi_1$  and  $\phi_2$  is shown in Figure 4B, overlaid with the X-ray structure of **25** for comparison. This conformation is also consistent with the NOE observed in NMR, since a pyrimidine methyl is within 5 Å of an ortho proton and the methyl protons are in the deshielding region of the ring.

As shown in Figure 4A, the transition state for rotation around  $\phi_2$  in **27** is approximately 7.5 kcal, about 6 kcal lower than the value obtained from variable-temperature experiments using the Eyring equation (Table 1).

In summary, we were able to show experimentally that the calculated conformations were in fact observed in solution and in crystals (with the exception of the asymmetric pyrimidine rotamer discussed above) and that low-energy conformations were well-separated energetically from other conformers. In addition, the studies suggest which functionality on the anilino pyrimidine is important for direct interaction with the receptor and which are important for presenting the correct conformation to the receptor (see below). This information was critical for the next step.

**Design of Conformationally Locked Mimetics.**

Rotational restriction around the central nitrogen of anilino pyrimidines is observed spectrally and is supported by calculations. Looking over the anilino pyrimidine SAR, steric hindrance of this rotation appears to

correlate crudely with potency: that is, the more rigidly locked conformations appear to be better antagonists. This same point was noted by Chen et al. in their SAR studies on anilino pyrimidines and -triazines.<sup>23</sup> The most striking example is the series of unsubstituted nitrogens and their *N*-methyl and *N*-ethyl congeners (previous paper), where *N*-H analogues are inactive unless large groups are present in the ortho positions (Chart 2). This result was encouraging since it suggested that the design of conformationally locked mimetics should be straightforward, provided that the unbound low-energy conformation we had deduced was similar to the receptor-bound conformation. The simplest way to mimic the calculated shape of, for example, **24**, is to restrict the rotation of the dihedral angle closest to 0°, as shown in Figure 5; since all of the atoms lie within 4° of a plane, they can be approximated by a planar aromatic ring. The literature indicated that the *N*-phenylpyrrolopyrimidine nucleus was accessible synthetically without difficulty (see Methods section). This core was initially chosen to test the proposed locked conformation. However, the key requirements of the core were only that

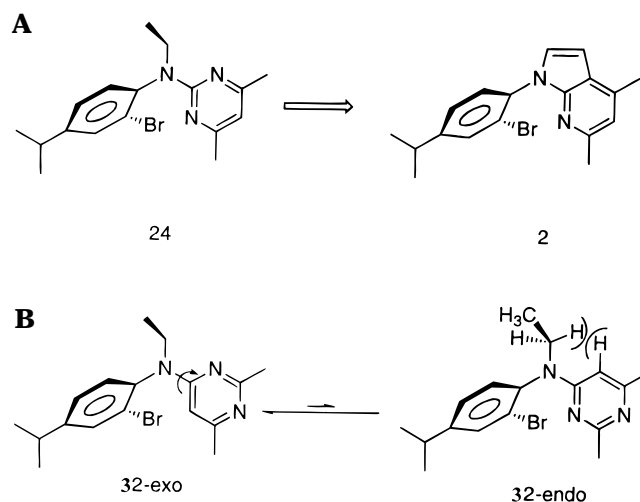


**Figure 5.** A. Locking of key dihedral  $\phi_2$  to form pyrrolopyrimidine. B. Postulated active (endo) and inactive conformations of isopyrimidine **32**. The absence of receptor affinity of **32** is suggested to be due to the predominance of the exo form in solution (see text for discussion).



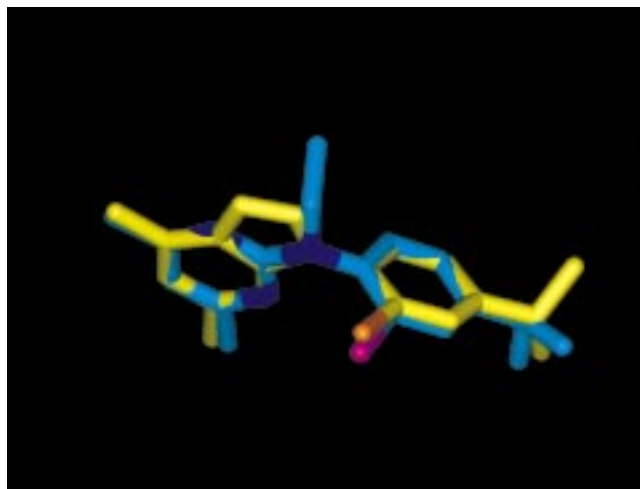


**Figure 6.** Crystal structure of conformationally locked pyrrolopyridine **2** (yellow carbons) overlaid with the calculated structure of anilinoypyrimidine **24** (cyan carbons).

the bicyclic system remain planar, the phenyl ring lie between  $60^\circ$  and  $90^\circ$  with respect to the bicyclic system, a lone pair acceptor lie on the inner face of the V-shaped molecule, and valency for the required substituents be available. Numerous variations on the position and number of nitrogens in the planar, bicyclo[4,3,0]-ring system were envisaged and subsequently shown to be active, as discussed in the next paper and references therein.

We next considered what the SARs in the anilinoypyrimidine series told us about the best groups to place on the constrained ring system. First, the anilinoypyrimidine maintains good potency with methyl groups in both the 4- and the 6-positions of the pyrimidine ring, so the dimethylpyrrolopyridine was a logical first choice (Figure 5A). Second, although we have constrained one degree of freedom, the phenyl ring on the pyrrole nitrogen still has a low barrier to rotation, and the SAR of anilinoypyrimidines indicated that this is an important factor. The aryl group in anilinoypyrimidine **24** was selected as the best test for the initial pyrrolopyridine, leading to **2**. The calculated low-energy geometries of these two molecules overlapped very closely (not shown; see Figure 6).

Third, the pyrrolopyridine replaces one of the pyrimidine ring nitrogens with the ring fusion carbon, resulting in the loss of this potential H-bond acceptor and alteration of the electronic character of the ring. The complete lack of antagonist potency of isopyrimidine **32** could be explained by the absence of a nitrogen in this position. However, NMR spectra of **32**, which show only two sharp, well-separated methyl peaks between  $-70$  and  $150^\circ\text{C}$ , provided an equally valid possibility: that the preferred solution conformation had the pyrimidine 2-nitrogen locked exo to the aromatic ring (Figure 5B), perhaps due to a higher barrier for rotation of the methine hydrogen past the *N*-ethyl group. The presence of only one rotamer of the isopyrimidine in the variable temperature NMR studies up to  $140^\circ\text{C}$  is also very strong support for this hypothesis (Table 1). These data and the SAR seemed to point toward the essential ring nitrogen being in the endo position; in any event, this hypothesis would be tested by the synthesis of pyrrolopyridine **2**.

The final point to be addressed by the SAR of the anilinoypyrimidines is the loss of the methyl group of the potent *N*-ethyl analogues. This methyl group projects above the plane of the new ring of **2** (Figure 5B), which would be difficult to mimic with a planar heterocycle. As in the ortho position of the aromatic ring, the conformational studies appeared to favor a locking role for the nitrogen substituent, rather than (or in addition to) a direct interaction with the receptor. Even if the extra carbon were important, the loss of the methyl group was not considered a serious flaw for the series since the *N*-methylanilinoypyrimidine is also moderately active. The additional carbon atom completing the five-membered ring occupies a space not filled by the anilinoypyrimidines, so its effect on binding was uncertain.

**Synthesis, Structure, and Biological Activity of Pyrrolopyridines.** The initial target **2** was selected for the reasons described above and also since the desired starting materials were readily synthesized. The synthetic routes are described in Methods and Experimental Section. The very first compound tested in the designed series proved to be active in the r-CRH<sub>1</sub> receptor-binding assay (**1**, 363 nM, Table 1). Removal of the cyano group improved the activity enough that we felt certain we had chosen the right conformer to mimic (**2**, 47 nM). Several correlations in the SAR with the anilinoypyrimidine SAR also gave us confidence: (a) removing the ortho substituent from the phenyl ring (**21**, 2462 nM) decreased activity; (b) substituting both phenyl ortho positions improved activity (**7**, 29 nM; **8**, 1 nM); and (c) placing a polar group on the central nitrogen substituent decreased activity (3-cyano analogues and the inactive 3-carboxamido and 3-carboxylate derivatives **22** and **23**).

Single-crystal X-ray structures of bicyclic inhibitors **2**, **3**, and **9** were obtained. An overlay of the X-ray structure of **2** with the calculated low-energy conformation of anilinoypyrimidine **24** is shown in Figure 6. The angle of the phenyl ring relative to the pyridine ring, the only significant degree of freedom remaining, is very close to the experimental and calculated values of anilinoypyrimidines. In addition, the crystal structure of **3** allowed regioisomeric assignment of the phenyl and methyl groups in **3** and **4** (see Methods and Supporting Information).

The high potency and close correlation of the structure and SAR with the original lead confirmed that we had developed an attractive new series with a defined binding mode. We could now use the fixed position of the pyrimidine ring substituents to confirm unambiguously the bound conformation of anilinoypyrimidines that we proposed from the spectral and SAR studies, as discussed above. Removing a methyl group from the 4-position resulted in a decrease in activity of about 5-fold (**11** vs **2**). Removal of the 6-methyl, however, caused a greater than 500-fold loss of activity (**12** vs **2**). This result shows that an *endo*-methyl is required for activity. Replacing the 6-methyl with the larger phenyl group (**3** vs **2**) also destroys activity, while a slight improvement is noticed in the 4-phenyl replacement (**4** vs **2**). Although the 6-morpholino compound was not prepared, analogous compounds in closely related series are less active.<sup>8</sup> The 4-morpholino derivatives **19** and

**20** retain potency. Replacing methyl with chloro in the 6-position causes only a 2-fold decrease in activity (**15**), suggesting that steric contacts are primarily responsible for the sensitivity of this site to substitution. These results clearly establish the *endo*-methyl conformation as the active conformation when the other ring substituent is large; again, this is not observed in the X-ray structure but appears to be present in solution (vide supra).

Comparison of the receptor-binding potency of the acyclic and cyclic series can be made in two ways: compounds **2** and **24** are identical homologues by number of carbon atoms and have effectively identical affinities (46 and 47 nM). On the other hand, the methyl group of **24** occupies a region that cannot be filled by **2**, and it might be argued that the acyclic *N*-methyl analogue **26** (96 nM) is a better comparator. In either case the effect of cyclization is relatively minor. It is not surprising that any entropy gain due to preorganization<sup>24</sup> would be small, given the restricted number of accessible states available to the acyclic compound.

The best compound, incorporating the potent 2-bromo-4,6-dimethoxyaryl group, binds to the r-CRH<sub>1</sub> receptor with an affinity of about 1 nM (**8**, Table 1). The compounds are selective for the human and rat CRH<sub>1</sub> receptor and do not bind with significant affinity to other common cell surface receptors (not shown).

## Conclusions

This report details a design and synthesis project that successfully yielded both a new series of antagonists and insight into the bound conformation of the original series. The original hypothesis—that free low-energy conformations were useful starting points for inferring a bound conformation—was validated for this series by the results. The first compound synthesized was active, and we attained equal potency with the lead series as well as structural novelty. The well-defined shape of the pharmacophore that resulted from the study also allowed the design of completely different scaffolds that will be described at a later time.

It is a fair critique to point out that these systems are simple, possess limited degrees of freedom, and therefore are ideal and perhaps predisposed to success in a study of this kind. In defense of taking the time to obtain an accurate initial understanding of the conformational preferences, however, it is important to reiterate several points that were made in the discussion: first, the choice of methods is crucial to success. This method should not be chosen to design mimetics of ligands with many equi-energetic minima and internal degrees of freedom unless resources are available to study them all systematically. The approach becomes much less efficient with shallow conformational energy surfaces, and this can be determined computationally at the outset. Second, even in this simple system there are many possible ways of conformational locking, and many chemist-months have been spent in unsuccessful attempts to mimic molecular shapes with “tied-up” or “tied-back” analogues without understanding the three-dimensional shape of the initial lead. In contrast, obtaining experimental and calculated structural information required just a few weeks of effort, and the synthesis of the initial pyrrolopyrimidine for proof of

principle required only 10–12 weeks by a single laboratory. Third, several methods (e.g., X-ray, variable-temperature NMR, and semiempirical calculations, in this case) are important to ensure a full understanding of the conformational preferences of the molecules to be mimicked; just an X-ray structure is frequently misleading. Finally, and most importantly, the design process depended heavily on the accurate SAR generated by chemists in the original lead series.

These bicyclic antagonists were subsequently extended to include a variety of other heterocyclic cores with promising CRH<sub>1</sub> receptor affinity, as described in the following paper.<sup>8</sup> Modification of the heterocycle and side chains to optimize potency, log *P*, solubility, oral availability, and CNS penetration led to the identification of compounds with properties that warrant further evaluation as potential clinically useful therapeutic agents.

## Experimental Section

**General.** All procedures were carried out under inert gas in oven-dried glassware unless otherwise indicated. Proton NMR spectra were obtained on VXR or Unity 300- or 400-MHz instruments (Varian Instruments, Palo Alto, CA) with TMS as an internal reference standard. Melting points were determined on a Mettler SP61 apparatus and are uncorrected. Elemental analyses were performed by Quantitative Technologies, Inc., Bound Brook, NJ. High-resolution mass spectra were carried out on a VG 70-VSE instrument with NH<sub>3</sub> chemical ionization. Thin layer and column chromatography were carried out on plates or silica gel from E. Merck, Darmstadt, FRG. Separation of optical isomers was performed using supercritical fluid chromatography with a Chiracel column (Daicel Chemical Ind. Ltd.) and 20% methanol modified CO<sub>2</sub> mobile phase. Optical rotations were obtained on a Perkin-Elmer 241 polarimeter. Solvents and reagents were obtained from commercial vendors in the appropriate grade and used without further purification unless otherwise indicated.

**1-(2-Bromo-4-isopropylphenyl)-3-cyano-4,6-dimethyl-7-azaindole (1).** **Part A.** A solution of 42.80 g (0.200 mol) of the potassium salt of formylsuccinonitrile<sup>25</sup> and 29.20 g (0.200 mol) of 2-bromo-4-isopropylaniline in a mixture of 50 mL of glacial acetic acid and 120 mL of ethanol was refluxed for 2 h. The mixture was stripped of most of the acetic acid and ethanol. The residue was taken up in ethyl acetate, washed with 10% sodium bicarbonate solution, dried with anhydrous sodium sulfate, and evaporated to give a dark, oily residue. This was chromatographed on silica gel with 80:20 hexanes–ethyl acetate to give 24.23 g (40%) of *N*-(2-bromo-4-isopropylphenyl)aminomethylenesuccinonitrile. MS: (M + NH<sub>4</sub>)<sup>+</sup> = 321.0; calcd, 321.0.

**Part B.** To a solution of 10 mL of 1 M potassium *tert*-butoxide in tetrahydrofuran and 10 mL of ethanol was added 1.11 g (3.65 mmol) of *N*-(2-bromo-4-isopropylphenyl)aminomethylenesuccinonitrile (part A), and the mixture was stirred for 16 h. The solvents were removed by evaporation. The residue was taken up in ethyl acetate and was washed successively with 1 N hydrochloric acid, 10% sodium bicarbonate solution, and brine. The solution was dried with anhydrous sodium sulfate and evaporated to give a dark residue. The residue was dissolved in dichloromethane, 20 g of silica gel was added, and the mixture was evaporated to dryness. This mixture was placed on top of a chromatographic column of 150 g of silica gel in hexane. The column was eluted successively with 10, 15, 20, 25, and 30% ethyl acetate in hexane to give 0.65 g (59% yield) of 1-(2-bromo-4-isopropylphenyl)-2-amino-4-cyanopyrrole. MS: (M + H)<sup>+</sup> = 304.0; calcd, 304.0. *R*<sub>f</sub> = 0.22 on silica gel thin-layer chromatography (70:30 hexanes–ethyl acetate). <sup>1</sup>H NMR (300 MHz, CDCl<sub>3</sub>) δ 7.58 (1H, d, *J* = 1.10 Hz), 7.29 (2H, m), 6.84 (1H, d, *J* = 1.46 Hz), 5.75 (1H, d, *J* = 1.56 Hz), 3.22 (2H, br s), 2.97 (6H, d, *J* = 6.96).



**Part C.** Parts A and B were scaled up for part C. A mixture of 18.51 g (0.0609 mol) of 1-(2-bromo-4-isopropylphenyl)-2-amino-4-cyanopyrrole, 300 mL of ethanol, 0.6 mL of concentrated hydrochloric acid, and 10 mL (9.75 g, 0.0974 mol) of 2,4-pentanedione was refluxed with stirring under a nitrogen atmosphere for 4 h. The mixture was allowed to cool, and the solvent was removed under reduced pressure. The residue was dissolved in ethyl acetate. The solution was washed with 10% sodium bicarbonate solution and then with brine. The solution was dried with anhydrous sodium sulfate and evaporated to give 21.76 g of dark, tarry residue. The residue was chromatographed on silica gel by eluting in step gradients of 0, 10, 15, 20, 25, and 30% ethyl acetate in hexane. The initial fraction was 17.6 g (78%) of 1-(2-bromo-4-isopropylphenyl)-3-cyano-4,6-dimethyl-7-azaindole, mp 108.2 °C. High-resolution MS:  $(M + H)^+ = 368.0749$ ; calcd, 368.0762 ( $^{79}\text{Br}$ ).  $R_f = 0.45$  on silica gel thin-layer chromatography with 70:30 hexanes-ethyl acetate.  $^1\text{H NMR}$  (300 MHz,  $\text{CDCl}_3$ )  $\delta$  7.73 (1H, s), 7.61 (1H, d,  $J = 1.47$  Hz), 7.40 (1H, d,  $J = 8.42$  Hz), 7.33 (1H, dd,  $J = 1.84, 8.43$  Hz), 6.93 (1H, s), 2.99 (1H, sept,  $J = 6.96$  Hz), 2.77 (3H, s), 2.53 (3H, s), 1.32 (6H, d,  $J = 6.96$  Hz). Anal. Calcd for  $\text{C}_{19}\text{H}_{18}\text{BrN}_3$ : C, 61.97; H, 4.93; N, 11.41. Found: C, 61.78; H, 4.91; N, 11.42.

**1-(2-Bromo-4-isopropylphenyl)-4,6-dimethyl-7-azaindole (2).** A mixture of 4.00 g of 1-(2-bromo-4-isopropyl)-3-cyano-4,6-dimethyl-7-azaindole and 40 mL of 65% sulfuric acid was refluxed for 1 h. The solution was cooled and poured onto ice. Concentrated ammonium hydroxide was added until the mixture was alkaline to pH paper. The mixture was extracted with ethyl acetate. The solution was dissolved in 60:40 hexanes-ethyl acetate and was passed through a short column of silica gel. The eluate was evaporated, and the residue was crystallized from 20 mL of hexane to give 2.45 g (66% yield) of 1-(2-bromo-4-isopropylphenyl)-4,6-dimethyl-7-azaindole, mp 76 °C. High-resolution MS:  $(M + H)^+ = 343.0818$ ; calcd, 343.0810.  $R_f = 0.57$  on silica gel (70:30 hexanes-ethyl acetate).  $^1\text{H NMR}$  (300 MHz,  $\text{CDCl}_3$ )  $\delta$  7.58 (1H, d,  $J = 1.83$  Hz), 7.43 (1H, d,  $J = 8.06$  Hz), 7.29 (1H, dd,  $J = 1.83, 8.06$  Hz), 7.23 (1H, d,  $J = 3.66$  Hz), 6.82 (1H, s), 6.59 (1H, d,  $J = 3.29$  Hz), 2.90 (1H, sept,  $J = 6.95$  Hz), 2.55 (3H, s), 2.54 (3H, s), 1.30 (6H, d,  $J = 6.96$  Hz). Anal. Calcd for  $\text{C}_{18}\text{H}_{19}\text{BrN}_2$ : C, 62.98; H, 5.58; N, 8.16. Found: C, 62.92; H, 5.60; N, 8.15.

**1-(2-Bromo-4-isopropylphenyl)-3-cyano-4-methyl-6-phenyl-7-azaindole (3) and (2-Bromo-4-isopropylphenyl)-3-cyano-6-methyl-4-phenyl-7-azaindole (4).** A mixture of 737 mg (2.00 mmol) of 1-(2-bromo-4-isopropylphenyl)-2-amino-4-cyanopyrrole (vide supra), 324 mg (2.00 mmol) of benzoylacetone, 10 mL of ethanol, and 0.025 mL of concentrated HCl was refluxed together for 48 h. The mixture was dissolved in dichloromethane-ethyl acetate and chromatographed on silica gel eluting in step gradients with 0, 5, 10, and 15% ethyl acetate in hexane to yield 1-(2-bromo-4-isopropylphenyl)-3-cyano-4-methyl-6-phenyl-7-azaindole, mp 130 °C (0.66 g, 77% yield) and 1-(2-bromo-4-isopropylphenyl)-3-cyano-6-methyl-4-phenyl-7-azaindole, mp 198 °C (0.02 g, 2% yield). The  $R_f$  values were respectively 0.38 and 0.28 (silica gel with 80:20 hexanes-ethyl acetate).

For the 4-methyl-6-phenyl compound:  $^1\text{H NMR}$  (300 MHz,  $\text{CDCl}_3$ )  $\delta$  7.98 (1H, d,  $J = 1.46$  Hz), 7.95 (1H, s), 7.85 (1H, s), 7.64 (1H, d,  $J = 1.47$  Hz), 7.53 (1H, s), 7.34-7.48 (5H, m), 3.01 (1H, sept,  $J = 6.98$  Hz), 2.88 (3H, s), 1.34 (6H, d,  $J = 6.96$  Hz). High-resolution MS:  $(M + H)^+ = 430.0901$ ; calcd, 430.0919.

For the isomeric 6-methyl-4-phenyl compound:  $^1\text{H NMR}$  (300 MHz,  $\text{CDCl}_3$ )  $\delta$  7.82 (1H, s), 7.64 (2H, 2s), 7.34-7.59 (6H, m), 7.14 (1H, s), 3.01 (1H, sept,  $J = 6.96$  Hz), 2.62 (3H, s), 1.33 (6H, d,  $J = 6.96$  Hz). High-resolution MS:  $(M + H)^+ = 430.0911$ ; calcd, 430.0919. Anal. Calcd for  $\text{C}_{24}\text{H}_{20}\text{BrN}_3$ : C, 67.31; H, 4.91; N, 9.57. Found: 67.20; H, 4.83; N, 9.53.

To improve the yield of the 4-phenyl isomer, 25 mL of xylene, 737 mg (2.00 mmol) of 1-(2-bromo-4-isopropylphenyl)-2-amino-4-cyanopyrrole (vide supra), and 324 mg (2.00 mmol) of benzoylacetone were heated in a flask equipped with a water

separator for 2 h. The solvent was removed by evaporation, and the residue was chromatographed on silica gel as described above to yield 138 mg (16%) of 1-(2-bromo-4-isopropylphenyl)-3-cyano-6-methyl-4-phenyl-7-azaindole (**4**), along with 350 mg of the 4-methyl-6-phenyl isomer (41%) and a substantial amount of unreacted pyrrole.

**1-(2-Bromo-4-isopropylphenyl)-6-methyl-4-phenyl-7-azaindole (5).** A mixture of 130 mg (0.302 mmol) of 1-(2-bromo-4-isopropylphenyl)-3-cyano-6-methyl-4-phenyl-7-azaindole (vide supra) and 10 mL of 65% sulfuric acid was refluxed for 1 h. The mixture was poured onto ice, and concentrated ammonium hydroxide was added until the mixture was basic to pH paper. The mixture was extracted with ethyl acetate. The extract was evaporated and chromatographed on silica gel with 70:30 hexanes-ethyl acetate. There was obtained 112 mg (92% yield) of 1-(2-bromo-4-isopropylphenyl)-6-methyl-4-phenyl-7-azaindole, mp 115 °C. High-resolution MS:  $(M + H)^+ = 405.0986$ ; calcd, 405.0966.  $^1\text{H NMR}$  (300 MHz,  $\text{CDCl}_3$ )  $\delta$  7.71 (1H, d,  $J = 1.83$  Hz), 7.68 (1H, d,  $J = 0.73$  Hz), 7.54 (1H, d,  $J = 0.73$  Hz), 7.35-7.48 (4H, m), 7.26 (1H, d,  $J = 1.83$  Hz), 7.23 (1H, d,  $J = 3.56$  Hz), 7.02 (1H, s), 6.68 (1H, d,  $J = 3.61$  Hz), 2.91 (1H, sept,  $J = 6.96$  Hz), 2.56 (3H, s), 1.25 (6H, d,  $J = 6.96$  Hz). Anal. Calcd for  $\text{C}_{23}\text{H}_{21}\text{BrN}_2$ : C, 68.15; H, 5.22; N, 6.76. Found: C, 67.73; H, 5.53; N, 6.38.

**1-(2-Bromo-4-isopropylphenyl)-4-methyl-6-phenyl-7-azaindole (6).** In the same way, 1-(2-bromo-4-isopropylphenyl)-4-methyl-6-phenyl-7-azaindole was obtained, mp 95.8 °C (82% yield).  $^1\text{H NMR}$  (300 MHz,  $\text{CDCl}_3$ )  $\delta$  8.01 (1H, d,  $J = 1.46$  Hz), 7.98 (1H, s), 7.62 (1H, d,  $J = 1.73$  Hz), 7.51 (1H, d,  $J = 8.05$  Hz), 7.29-7.43 (6H, m), 6.66 (1H, d,  $J = 3.66$  Hz), 2.99 (1H, sept,  $J = 6.96$  Hz), 2.66 (3H, s), 1.32 (6H, d,  $J = 6.96$  Hz). High-resolution MS:  $(M + H)^+ = 405.0972$ ; calcd, 405.0966. Anal. Calcd for  $\text{C}_{22}\text{H}_{21}\text{BrN}_2$ : C, 68.15; H, 5.22; N, 6.91. Found: C, 68.22; H, 5.46; N, 6.54.

**1-(2-Bromo-4,6-dimethoxyphenyl)-3-cyano-4,6-dimethyl-7-azaindole (7).** **Part A.** *N*-(2-bromo-4,6-dimethoxyphenyl)-aminomethylenesuccinonitrile was prepared from 2-bromo-4,6-dimethoxyaniline by the method described for *N*-(2-bromo-4-isopropylphenyl)aminomethylenesuccinonitrile (vide supra). MS:  $(M + H)^+ = 322.0$ ; calcd, 322.16 ( $^{79}\text{Br}$ ).  $R_f = 0.19$  (silica gel with 60:40 hexanes-ethyl acetate).

**Part B.** The product from part A was cyclized with potassium *tert*-butoxide as described above for the cyclization of *N*-(2-bromo-4-isopropylphenyl)aminomethylenesuccinonitrile to give 1-(2-bromo-4,6-dimethoxyphenyl)-2-amino-4-cyanopyrrole, mp 161 °C, in 79% yield.  $R_f = 0.19$  (silica gel with 60:40 hexanes-ethyl acetate). High-resolution MS:  $(M + H)^+ = 321.0095$ ; calcd, 321.0113.  $^1\text{H NMR}$  (300 MHz,  $\text{CDCl}_3$ )  $\delta$  6.82 (1H, d,  $J = 2.56$  Hz), 6.76 (1H, d,  $J = 2.83$  Hz), 6.53 (1H, d,  $J = 2.56$  Hz), 5.76 (1H, d,  $J = 2.83$  Hz), 3.85 (3H, s), 3.79 (3H, s), 3.13 (2H, br s).

**Part C.** The product from part B was treated with 2,4-pentanedione as described above for the preparation 1-(2-bromo-4-isopropylphenyl)-3-cyano-4,6-dimethyl-7-azaindole to give 1-(2-bromo-4,6-dimethoxyphenyl)-3-cyano-4,6-dimethyl-7-azaindole, mp 186 °C, in 92% yield. MS:  $(M + H)^+ = 388.0$ ; calcd, 388.0.  $R_f = 0.44$  (silica gel with 60:40 hexanes-ethyl acetate).  $^1\text{H NMR}$  (300 MHz,  $\text{DMSO}-d_6$ )  $\delta$  8.37 (1H, s), 7.03 (1H, s), 7.01 (1H, d,  $J = 2.56$  Hz), 6.84 (1H, d,  $J = 2.20$  Hz), 3.89 (3H, s), 3.69 (3H, s), 2.67 (3H, s), 2.41 (3H, s). Anal. Calcd for  $\text{C}_{18}\text{H}_{16}\text{BrN}_3\text{O}_2$ : C, 55.97; H, 4.19; N, 10.88. Found: C, 55.79; H, 4.09; N, 10.65.

**1-(2-Bromo-4,6-dimethoxyphenyl)-4,6-dimethyl-7-azaindole (8).** A mixture of 200 mg of 1-(2-bromo-4,6-dimethoxyphenyl)-3-cyano-4,6-dimethyl-7-azaindole and 10 mL of 65% sulfuric acid was refluxed for 1 h. The mixture was worked up as described above for other decyanylations in this series to give 185 mg of crude product. MS of this crude material showed  $(M + H)^+ = 361.0$  (major), 347.0, and 330.0. These numbers suggest that some mono- and bis-*O*-demethylation accompanied the decyanylation procedure. A 40-mg portion was purified by preparative HPLC on a nitrile column using 95:5 1-chlorobutane-acetonitrile to give 11 mg of 1-(2-bromo-4,6-dimethoxyphenyl)-4,6-dimethyl-7-azaindole. High-resolu-

tion MS:  $(M + H)^+ = 360.0479$ ; calcd, 360.0473. A better solution to the attendant O-demethylation was found: the crude reaction mixture (175 mg, 0.5 mmol) was remethylated by stirring the mixture with lithium bis(trimethylsilylamide) (2.28 g, 16.1 mmol) and methyl iodide (2.5 mmol, 1 M in THF) in tetrahydrofuran (10 mL) for 16 h. The resulting product could then be purified relatively easily by preparative thin-layer chromatography on silica gel with 95:5 methylene chloride–methanol ( $R_f$  0.31). Finally, the product was crystallized from methanol to give crystals (32 mg) of the dimethoxy compound, mp 202 °C.  $^1\text{H NMR}$  (300 MHz,  $\text{CDCl}_3$ )  $\delta$  7.02 (1H, d,  $J = 3.66$  Hz), 6.85 (1H, d,  $J = 2.56$  Hz), 6.78 (1H, s), 6.60 (1H, d,  $J = 3.66$  Hz), 6.56 (1H, d,  $J = 2.56$  Hz), 3.86 (3H, s), 3.68 (3H, s), 2.54 (3H, s), 2.51 (3H, s). Anal. Calcd for  $\text{C}_{17}\text{H}_{17}\text{BrN}_2\text{O}_2$ : C, 56.52; H, 4.78; N, 7.75. Found: C, 56.69; H, 4.38; N, 7.58.

**1-(2-Bromo-4-isopropylphenyl)-3-cyano-6-methyl-7-azaindole (9) and 1-(2-Bromo-4-isopropylphenyl)-3-cyano-4-methyl-7-azaindole (10).** To a solution of 1.085 g (5.07 mmol) of 1-(2-bromo-4-isopropylphenyl)-2-amino-4-cyanopyrrole and 0.80 mL (0.797 g, 6.03 mmol) of acetoacetaldehyde dimethyl acetal in 20 mL of ethanol was added 0.10 mL of concentrated hydrochloric acid. The mixture was refluxed for 16 h. The mixture was cooled and evaporated to give a dark, thick oil. TLC on silica gel with 70:30 hexanes–ethyl acetate showed two major spots at  $R_f$  0.47 and 0.41. The oil was dissolved in ethyl acetate, 20 mL silica gel powder was added, and the mixture was evaporated to dryness. The powdery residue was loaded on top of a column of 60 mL of silica gel in hexane. The column was eluted in step gradients of 0, 5, 10, 15, 20, and 25% ethyl acetate in hexane. The first fraction to elute was 0.32 g of 1-(2-bromo-4-isopropylphenyl)-3-cyano-6-methyl-7-azaindole,  $R_f$  0.47 (silica gel with 70:30 hexanes–ethyl acetate). The material was crystallized from hexane to give 176 mg (10%) of crystals, mp 125 °C. High-resolution MS:  $(M + H)^+ = 354.0603$ ; calcd, 354.0606.  $^1\text{H NMR}$  (300 MHz,  $\text{CDCl}_3$ )  $\delta$  8.01 (1H, d,  $J = 8.06$  Hz), 7.76 (1H, s), 7.62 (1H, d,  $J = 1.83$  Hz), 7.41 (1H, d,  $J = 8.06$  Hz), 7.34 (1H, dd,  $J = 1.83, 8.42$  Hz), 7.17 (1H, d,  $J = 8.06$  Hz), 3.00 (1H, sept,  $J = 6.96$  Hz), 2.60 (3H, s), 1.32 (6H, d,  $J = 6.96$  Hz). Anal. Calcd for  $\text{C}_{18}\text{H}_{16}\text{BrN}_3$ : C, 61.03; H, 4.55; N, 11.86. Found: C, 60.97; H, 4.48; N, 11.84.

The second fraction to elute was 180 mg (after recrystallization from hexane) (10%) of 1-(2-bromo-4-isopropylphenyl)-3-cyano-4-methyl-7-azaindole, mp 176.0 °C,  $R_f$  0.4. MS:  $(M + H)^+ = 354.0595$ ; calcd, 354.0606.  $^1\text{H NMR}$  (300 MHz,  $\text{CDCl}_3$ )  $\delta$  8.31 (1H, d,  $J = 4.76$  Hz), 7.82 (1H, s), 7.63 (1H, d,  $J = 1.83$  Hz), 7.40 (1H, d,  $J = 8.06$  Hz), 7.36 (1H, dd,  $J = 1.83, 8.42$  Hz), 7.07 (1H, dd,  $J = 0.73, 4.76$  Hz), 2.99 (1H, sept,  $J = 6.96$  Hz), 2.84 (3H, s), 1.31 (6H, d,  $J = 6.96$  Hz). Anal. Calcd for  $\text{C}_{18}\text{H}_{16}\text{BrN}_3$ : C, 61.03; H, 4.55; N, 11.86. Found: C, 61.00; H, 4.39; N, 11.86.

**1-(2-Bromo-4-isopropylphenyl)-6-methyl-7-azaindole (11).** Compound 9 was decyanylated with 65% sulfuric acid as described above to give the desired product as a viscous oil. TLC on silica gel with 70:30 hexanes–ethyl acetate showed  $R_f = 0.57$ . High-resolution MS:  $(M + H)^+ = 329.0641$ ; calcd, 329.0653 ( $^{79}\text{Br}$ ).  $^1\text{H NMR}$  (300 MHz,  $\text{CDCl}_3$ )  $\delta$  7.84 (1H, d,  $J = 8.06$  Hz), 7.58 (1H, d,  $J = 1.83$  Hz), 7.44 (1H, d,  $J = 8.06$  Hz), 7.29 (1H, dd,  $J = 1.83, 8.06$  Hz), 7.24 (1H, d,  $J = 3.66$  Hz), 6.99 (1H, d,  $J = 8.06$  Hz), 6.56 (1H, d,  $J = 3.30$  Hz), 2.96 (1H, sept,  $J = 6.96$  Hz), 2.58 (3H, s), 1.30 (6H, d,  $J = 6.96$  Hz). Anal. Calcd  $\text{C}_{17}\text{H}_{17}\text{BrN}_2\text{H}_2\text{O}$ : C, 58.80; H, 5.52; N, 8.07. Found: C, 58.50; H, 4.93; N, 8.07.

**1-(2-Bromo-4-isopropylphenyl)-4-methyl-7-azaindole (12).** Compound 10 was decyanylated with 65% sulfuric acid as described above to give the desired product as a viscous oil. TLC on silica gel with 70:30 hexanes–ethyl acetate showed  $R_f = 0.48$ . High-resolution MS:  $(M + H)^+ = 329.0633$ ; calcd, 329.0653 ( $^{79}\text{Br}$ ).  $^1\text{H NMR}$  (300 MHz,  $\text{CDCl}_3$ ):  $\delta$  8.22 (1H, d,  $J = 4.76$  Hz), 7.60 (1H, d,  $J = 1.83$  Hz), 7.41 (1H, d,  $J = 8.06$  Hz), 7.29–7.33 (2H, m), 6.93 (1H, d,  $J = 4.76$  Hz), 6.65 (1H, d,  $J = 3.60$  Hz), 2.97 (1H, sept,  $J = 6.96$  Hz), 2.61 (3H, s), 1.30 (6H, d,  $J = 6.96$  Hz).

**1-(2-Bromo-4-isopropylphenyl)-6-hydroxy-3-cyano-4-methyl-7-azaindole (13) and 1-(2-Bromo-4-isopropylphenyl)-6-chloro-3-cyano-4-methyl-7-azaindole (14).** Part A. A solution of 3.04 g of 1-(2-bromo-4-isopropylphenyl)-2-amino-4-cyanopyrrole, 1.9 mL (1.94 g, 14.9 mmol) of ethyl acetoacetate, and 0.1 mL of concentrated hydrochloric acid in 30 mL of ethanol was refluxed for 16 h. A precipitate formed upon cooling. The precipitate was removed by filtration to give 1.68 g of crystals, mp 202 °C, of 1-(2-bromo-4-isopropylphenyl)-4-methyl-7-azaindol-6-one. TLC on silica gel with 70:30 hexanes–ethyl acetate showed a single spot,  $R_f = 0.29$ . MS:  $(M + H)^+ = 370.0$ ; calcd, 370.05 ( $^{79}\text{Br}$ ).  $^1\text{H NMR}$  (300 MHz,  $\text{CDCl}_3$ )  $\delta$  7.60 (1H, d,  $J = 0.73$  Hz), 7.48, (1H, s), 7.30 (2H, 2s), 6.21 (1H, d,  $J = 0.73$  Hz), 3.03 (1H, sept,  $J = 6.96$  Hz), 2.70 (3H, s), 1.35 (6H, d,  $J = 6.96$  Hz).

**Part B.** A mixture of 185 mg of the 7-azaindol-6-one (part A) and 50 mL of phosphorus oxychloride was heated in an autoclave at 180 °C for 10 h. The excess phosphorus oxychloride was removed by distillation at reduced pressure. The residue was distributed between ethyl acetate and water. The ethyl acetate layer was separated and washed with 10% sodium bicarbonate solution and then with brine. The solution was dried ( $\text{Na}_2\text{SO}_4$ ) and evaporated. TLC of the residue on silica gel with 70:30 hexanes–ethyl acetate showed a major new product,  $R_f = 0.52$  with minor spots at  $R_f$  0.45 and 0.29. Chromatography on silica gel with step gradients of 5, 10, 15, and 20% ethyl acetate in hexane gave 109 mg (56%) of the  $R_f$  0.52 product, 1-(2-bromo-4-isopropylphenyl)-6-chloro-3-cyano-4-methyl-7-azaindole, mp 124 °C.  $^1\text{H NMR}$  (300 MHz,  $\text{CDCl}_3$ )  $\delta$  7.79 (1H, d,  $J = 5.13$  Hz), 7.60 (1H, d,  $J = 1.83$  Hz), 7.28–7.44 (2H, m), 7.11 (1H, s), 2.99 (1H, sept,  $J = 6.96$  Hz), 2.81 (3H, s), 1.31 (6H, d,  $J = 6.59$  Hz). Anal. Calcd for  $\text{C}_{18}\text{H}_{15}\text{BrClN}_3$ : C, 55.62; H, 3.90; N, 10.81; Cl, 9.12. Found: C, 57.80; H, 4.10; N, 10.89; Cl, 12.17.

**1-(2-Bromo-4-isopropylphenyl)-6-chloro-4-methyl-7-azaindole (15).** A mixture of 52 mg of 1-(2-bromo-4-isopropylphenyl)-6-chloro-3-cyano-4-methyl-7-azaindole and 10 mL of 65% sulfuric acid was refluxed for 1 h. The cooled solution was poured onto ice, and 17 mL of concentrated ammonium hydroxide was added. The alkaline mixture was extracted with ethyl acetate. The extract was washed (brine), dried ( $\text{Na}_2\text{SO}_4$ ), and evaporated. TLC of the residue on silica gel with 70:30 hexanes–ethyl acetate showed a major new spot,  $R_f = 0.58$ , with a trace of unchanged starting material ( $R_f$  0.52). The crude product was purified by preparative TLC on silica gel with 70:30 hexanes–ethyl acetate to give 39 mg (79% yield) of product, which slowly crystallized on standing, mp 75 °C. High-resolution MS:  $(M + H)^+ = 363.0247$ ; calcd, 363.0264 ( $^{79}\text{Br}$ ,  $^{35}\text{Cl}$ ). Anal. Calcd for  $\text{C}_{17}\text{H}_{16}\text{BrClN}_2\text{O}\cdot 0.14\text{C}_6\text{H}_{14}$ : C, 57.03; H, 4.82; N, 7.46. Found: C, 57.42; H, 4.54; N, 7.52.

**1-(2-Bromo-4-isopropylphenyl)-3-cyano-6-methyl-7-azaindole 7-N-Oxide (16) and 1-(2-Bromo-4-isopropylphenyl)-4-chloro-3-cyano-6-methyl-7-azaindole (17).** Part A. A solution of 1.24 g of 1-(2-bromo-4-isopropylphenyl)-3-cyano-6-methyl-7-azaindole (vide supra) and 1.42 g of 85% 3-chloroperoxybenzoic acid in 20 mL of chloroform was refluxed for 6 h. The mixture was cooled and washed first with 10% sodium bicarbonate solution and then with brine. The solution was dried ( $\text{Na}_2\text{SO}_4$ ) and evaporated. TLC of the residue on silica gel with 95:5 dichloromethane–methanol showed a trace spot at  $R_f$  0.88 and a major spot at  $R_f$  0.34. The material was purified by chromatography on silica gel with dichloromethane, followed by 1% methanol in dichloromethane, to give a trace of unchanged 1-(2-bromo-4-isopropylphenyl)-3-cyano-6-methyl-7-azaindole ( $R_f$  0.88) and 0.92 g (71%) of 1-(2-bromo-4-isopropylphenyl)-3-cyano-6-methyl-7-azaindole 7-oxide ( $R_f$  0.34), mp 179 °C. High-resolution MS:  $(M + H)^+ = 370.0559$ ; calcd, 370.0555 ( $^{79}\text{Br}$ ).  $^1\text{H NMR}$  (300 MHz,  $\text{CDCl}_3$ )  $\delta$  7.64 (1H, d,  $J = 8.43$  Hz), 7.54 (2H, m), 7.42 (1H, d,  $J = 8.05$  Hz), 7.29 (1H, dd,  $J = 1.83, 8.05$  Hz), 7.24 (1H, d,  $J = 8.06$  Hz), 2.98 (1H, sept,  $J = 6.96$  Hz), 2.58 (3H, s), 1.30 (6H, d,  $J = 6.59$  Hz). Anal. Calcd for  $\text{C}_{18}\text{H}_{16}\text{BrN}_3\text{O}$ : C, 58.39; H, 4.36; N, 11.35. Found: C, 58.15; H, 4.17; N, 11.22.



**Part B.** A mixture of 370 mg of the 7-oxide (part A) and 5 mL of phosphorus oxychloride was refluxed for 2 h. The solution was cooled, poured on ice, and stirred until most of the phosphorus oxychloride had hydrolyzed. The mixture was made alkaline with concentrated ammonium hydroxide and was extracted with ethyl acetate. The extract was dried ( $\text{Na}_2\text{SO}_4$ ) and evaporated to give a viscous residue. TLC on silica gel with 95:5 dichloromethane–methanol showed a major spot at  $R_f = 0.79$ . The material was purified by preparative TLC on silica gel with 70:30 hexanes–ethyl acetate to give crystals. Recrystallization from hexane gave 158 mg (41%) of 1-(2-bromo-4-isopropylphenyl)-4-chloro-3-cyano-6-methyl-7-azaindole, mp 123 °C. High-resolution MS:  $(M + H)^+ = 388.0197$ ; calcd, 388.0216 ( $^{79}\text{Br}$ ,  $^{35}\text{Cl}$ ).  $^1\text{H NMR}$  (300 MHz,  $\text{CDCl}_3$ )  $\delta$  7.79 (1H, s), 7.62 (1H, d,  $J = 1.47$  Hz), 7.35 (2H, m), 7.16 (1H, s), 3.00 (1H, sept,  $J = 6.96$  Hz), 2.56 (3H, s), 1.32 (6H, d,  $J = 6.96$  Hz). Anal. Calcd for  $\text{C}_{18}\text{H}_{15}\text{ClBrN}_3$ : C, 55.62; H, 3.90; N, 10.81. Found: C, 55.67; H, 3.81; N, 10.70.

**1-(2-Bromo-4-isopropylphenyl)-4-chloro-6-methyl-7-azaindole (18).** A mixture of 190 mg of compound 17 and 5 mL of 65% sulfuric acid was refluxed for 30 min. The solution was poured onto ice and extracted with ethyl acetate. The extract was washed with brine, dried ( $\text{Na}_2\text{SO}_4$ ), and evaporated. TLC of the residue on silica gel with 60:40 hexanes–ethyl acetate showed a major spot at  $R_f = 0.67$ . The residue was purified by preparative TLC to give 130 mg (73%) of viscous oil, 1-(2-bromo-4-isopropylphenyl)-4-chloro-6-methyl-7-azaindole. High-resolution MS:  $(M + H)^+ = 363.0246$ ; calcd, 363.0264 ( $^{79}\text{Br}$ ,  $^{35}\text{Cl}$ ).  $^1\text{H NMR}$  (300 MHz,  $\text{CDCl}_3$ )  $\delta$  7.59 (1H, d,  $J = 1.83$  Hz), 7.40 (1H, d,  $J = 8.06$  Hz), 7.30 (1H, dd,  $J = 1.83$ , 8.06 Hz), 7.27 (1H, d,  $J = 4.03$  Hz), 7.03 (1H, s), 6.66 (1H, d,  $J = 3.66$  Hz), 2.98 (1H, sept,  $J = 6.96$  Hz), 2.55 (3H, s), 1.31 (6H, d,  $J = 6.96$  Hz). Anal. Calcd for  $\text{C}_{17}\text{H}_{16}\text{ClBrN}_2 \cdot 0.33\text{H}_2\text{O}$ : C, 55.34; H, 4.51; N, 7.59. Found: C, 55.36; H, 4.13; N, 7.38.

**1-(2-Bromo-4-isopropylphenyl)-3-cyano-6-methyl-4-(1-morpholino)-7-azaindole (19).** A solution of 100 mg of 1-(2-bromo-4-isopropylphenyl)-3-cyano-6-methyl-7-azaindole 7-oxide in 5 mL of chloroform was treated with 0.10 mL (168 mg) of trifluoromethanesulfonic anhydride. The mixture was stirred at room temperature for 20 min. Anhydrous morpholine (0.20 mL, 200 mg) was added, and the mixture was refluxed for 2 h. The mixture was distributed between ethyl acetate and 10% aqueous  $\text{NaHCO}_3$ . The organic layer was washed with brine, dried ( $\text{Na}_2\text{SO}_4$ ), and evaporated to give 116 mg (98%) of solid. Recrystallization from ethanol gave 74 mg of crystalline 1-(2-bromo-4-isopropylphenyl)-3-cyano-6-methyl-4-(1-morpholino)-7-azaindole, mp 192 °C. TLC on silica gel with 60:40 hexanes–ethyl acetate showed one spot,  $R_f$  0.42. High-resolution MS:  $(M + H)^+ = 441.1099$ ; calcd, 441.1113 ( $^{81}\text{Br}$ ).  $^1\text{H NMR}$  (300 MHz,  $\text{CDCl}_3$ )  $\delta$  7.69 (1H, s), 7.61 (1H, d,  $J = 1.83$  Hz), 7.39 (1H, d,  $J = 1.83$  Hz), 7.33 (1H, dd,  $J = 1.83$ , 8.06 Hz), 6.56 (1H, s), 4.02 (4H, tr,  $J = 4.39$  Hz), 3.33 (4H, tr,  $J = 4.39$  Hz), 2.99 (1H, sept,  $J = 6.96$  Hz), 2.52 (3H, s), 1.31 (6H, d,  $J = 6.95$  Hz). Anal. Calcd for  $\text{C}_{22}\text{H}_{23}\text{BrN}_4\text{O}$ : C, 60.14; H, 5.28; N, 12.75; Br, 18.19. Found: C, 60.14; H, 5.26; N, 12.57; Br, 18.37.

**1-(2-Bromo-4-isopropylphenyl)-6-methyl-4-(1-morpholino)-7-azaindole (20).** A mixture of 48 mg of 1-(2-bromo-4-isopropylphenyl)-3-cyano-6-methyl-4-(1-morpholino)-7-azaindole and 5 mL of 65% sulfuric acid was refluxed for 45 min. The solution was poured into ice water. The solution was made alkaline with 10 mL of concentrated ammonium hydroxide, and a precipitate formed. Ethyl acetate was added, and the precipitate dissolved upon stirring. The organic extract was washed with brine, dried ( $\text{Na}_2\text{SO}_4$ ), and evaporated to give 46 mg of crystalline residue. TLC of the residue on silica gel with 60:40 hexanes–ethyl acetate showed a major spot at  $R_f = 0.36$ . The major component was isolated by preparative TLC of silica gel using 50:50 hexanes–ethyl acetate to give 33 mg (73% yield) of product. Recrystallization from hexane gave 19 mg of crystals of 1-(2-bromo-4-isopropylphenyl)-6-methyl-4-(1-morpholino)-7-azaindole, mp 100 °C.  $^1\text{H NMR}$  (300 MHz,  $\text{CDCl}_3$ )  $\delta$  7.58 (1H, d,  $J = 1.8$  Hz), 7.41 (1H, d,  $J = 8.1$  Hz), 7.29 (1H, dd,  $J = 1.8$ , 8.1 Hz), 7.12 (1H, d,  $J = 3.7$  Hz), 6.54

(1H, d,  $J = 3.7$  Hz), 6.37 (1H, s), 3.94 (4H, t,  $J = 4.8$  Hz), 3.46 (4H, t,  $J = 4.8$  Hz), 2.96 (1H, sept,  $J = 6.8$  Hz), 2.51 (3H, s), 1.30 (7H, d,  $J = 6.6$  Hz). High-resolution MS:  $(M + H)^+ = 416.1152$ ; calcd, 416.1161. Anal. Calcd for  $\text{C}_{21}\text{H}_{24}\text{BrN}_3\text{O}$ : C, 60.87; H, 5.84; N, 10.14. Found: C, 60.83; H, 5.96; N, 10.08.

**1-(4-Isopropylphenyl)-4,6-dimethyl-7-azaindole (21).** A mixture of 250 mg (0.729 mmol) of 1-(2-bromo-4-isopropyl)-4,6-dimethyl-7-azaindole, 20 mL of acetic acid, and 50 mg of 10% Pd on carbon was hydrogenated for 16 h at atmospheric pressure. The catalyst was filtered off, and the filtrate was evaporated on a rotary evaporator. The residue was dissolved in ethyl acetate and washed first with 10% aqueous  $\text{NaHCO}_3$  and then brine. The solution was dried ( $\text{Na}_2\text{SO}_4$ ) and evaporated to give 0.20 g (100%) of 1-(4-isopropylphenyl)-4,6-dimethyl-7-azaindole, an oil. High-resolution MS:  $(M + H)^+ = 265.1693$ ; calcd, 265.1705.  $^1\text{H NMR}$  (300 MHz,  $\text{CDCl}_3$ )  $\delta$  7.70 (2H, d,  $J = 8.8$  Hz), 7.38 (1H, d,  $J = 3.7$  Hz), 7.34 (2H, d,  $J = 8.4$  Hz), 6.82 (1H, s), 6.57 (1H, d,  $J = 3.7$  Hz), 2.96 (1H, sept,  $J = 6.9$  Hz), 2.59 (3H, s), 2.54 (3H, s), 1.29 (6H, d,  $J = 7.0$  Hz). Anal. Calcd for  $\text{C}_{18}\text{H}_{20}\text{N}_2 \cdot 0.5\text{H}_2\text{O}$ : C, 79.08; H, 7.74; N, 10.25. Found: C, 79.24; H, 7.50; N, 10.03.

**1-(2-Bromo-4-isopropylphenyl)-3-carboxamido-4,6-dimethylazaindole (22).** To a stirred solution of 1.10 g of 1-(2-bromo-4-isopropylphenyl)-3-cyano-4,6-dimethyl-7-azaindole in 2.5 mL of dimethyl sulfoxide were added 1.00 g (7.2 mmol) of pulverized anhydrous  $\text{K}_2\text{CO}_3$  and 5 mL (5.55 g, 1.67 g net, 48.9 mmol) of 30%  $\text{H}_2\text{O}_2$  in portions. The mixture frothed. It was allowed to stir 16 h at room temperature. The mixture was added to a mixture of ethyl acetate and water. The EtOAc layer was separated and washed again with water and then with brine. The solution was dried ( $\text{Na}_2\text{SO}_4$ ) and evaporated to give 1.03 g (89%) of crystals, mp 237 °C. Thin-layer chromatography on silica gel (95:5 methylene chloride–methanol) showed one spot,  $R_f$  0.22. MS:  $(M + H)^+ = 386.1$ ; calcd, 386.1.  $^1\text{H NMR}$  (300 MHz,  $\text{DMSO}-d_6$ )  $\delta$  7.95 (1H, s), 7.74 (1H, s), 7.54 (1H, br), 7.46 (2H, 2s), 7.03 (1H, br), 6.92 (1H, s), 3.05 (1H, sept,  $J = 6.96$  Hz), 2.72 (3H, s), 2.39 (3H, s), 1.28 (6H, d,  $J = 6.96$  Hz).

**1-(2-Bromo-4-isopropylphenyl)-3-carboxyl-4,6-dimethyl-7-azaindole (23).** A solution of 772 mg (2.00 mmol) of 1-(2-bromo-4-isopropylphenyl)-3-carboxamido-4,6-dimethyl-7-azaindole and 500 mg (425 mg net, 7.57 mmol) of 85% KOH in 10 mL of diethylene glycol was heated at 225 °C for 2 h. The solution was partially cooled and poured into 100 mL of water. The solution was filtered to remove a trace of cloudiness. Addition of 1 N HCl gave a precipitate, which was filtered off, washed with water, and dried to give 713 mg of light gray solid. The solid was chromatographed on silica gel by eluting with 1% methanol–methylene chloride. There was obtained 507 mg (65%) of crystals, mp 242 °C dec. MS:  $(M + H)^+ = 387.0$ ; calcd, 387.1.  $^1\text{H NMR}$  (300 MHz,  $\text{DMSO}-d_6$ )  $\delta$  8.11 (1H, s), 7.74 (1H, d,  $J = 2.03$  Hz), 7.44–7.51 (2H, m), 6.97 (1H, s), 3.03 (1H, sept,  $J = 6.96$  Hz), 2.79 (3H, s), 2.39 (3H, s), 1.28 (6H, d,  $J = 6.96$ ).

**Supporting Information Available:** X-ray crystal data, descriptions of data collection, treatment, solution, and refinement, and tables of fractional coordinates and isotropic and anisotropic thermal parameters for compounds 2, 3, 9, 25, and 29. This information is available free of charge via the Internet at <http://pubs.acs.org>.

## References

- Arvanitis, A.; Gilligan, P. J.; Chorvat, R. J.; Cheeseman, R. S.; Christos, T. E.; Bajthavatchalam, R.; Beck, J. P.; Cocuzza, A. J.; Hobbs, F. W.; Trainor, G. L.; Wilde, R. G.; Arnold, C.; Chidester, D.; Curry, M.; He, L.; Hollis, A.; Klaczkiwicz, J.; Krinitsky, P. J.; Rescinito, J. P.; Scholfield, E.; Culp, S.; DeSouza, E. B.; Fitzgerald, L.; Grigoriadis, D.; Tam, W. S.; Wong, N.; Huang, S.; Shen, H. Non-Peptide Corticotropin-Releasing Hormone Antagonists: Syntheses and Structure–Activity Relationships of 2-Anilinopyrimidines and -triazines. *J. Med. Chem.* **1999**, *42*, 805–818.
- Pauletti, G. M.; Gangwar, S.; Siahaan, T. J.; Aube, J.; Borchardt, R. T. Improvement of Oral Peptide Bioavailability: Peptidomimetics and Prodrug Strategies. *Adv. Drug Delivery Rev.* **1997**, *27* (2, 3), 235–256.

- (3) Begley, D. J. The Blood-Brain Barrier: Principles for Targeting Peptides and Drugs to the Central Nervous System. *J. Pharm. Pharmacol.* **1996**, *48* (2), 136–146.
- (4) Strader, C. D.; Fong, T. M.; Tota, M. R.; Underwood, D. J.; Dixon, R. A. F. Structure and Function of G-protein-coupled Receptors. *Annu. Rev. Biochem.* **1994**, *63*, 101–132.
- (5) Rivier, J.; Rivier, C.; Vale, W. Synthetic Competitive Antagonists of Corticotropin-Releasing Factor: Effect On ACTH Secretion In the Rat. *Science* **1984**, *224* (4651), 889–891.
- (6) Sugg, E. E. Nonpeptide Agonists for Peptide Receptors. Lessons from Ligands. *Annu. Rep. Med. Chem.* **1997**, *32*, 277–283.
- (7) Babine, R. E.; Bender, S. L. Molecular Recognition of Protein-Ligand Complexes: Applications to Drug Design. *Chem. Rev.* **1997**, *97* (5), 1359–1472.
- (8) Chorvat, R. J.; Bakthavatchalam, R.; Beck, J. P.; Gilligan, P. J.; Wilde, R. G.; Cocuzza, A.; Hobbs, F. W.; Cheeseman, R. S.; Curry, M.; Rescinito, J. P.; Krenitsky, P.; Chidester, D.; Yarem, J.; Klackewicz, J. D.; Hodge, C. N.; Aldrich, P. E.; Wasserman, Z. R.; Fernandez, C. H.; Zaczek, R.; Fitzgerald, L.; Huang, S.-M.; Shen, H. L.; Wong, Y. N.; Chien, B. M.; Quon, C. Y.; Arvanitis, A. Synthesis, Corticotropin-Releasing Factor Receptor Binding Affinity, and Pharmacokinetic Properties of Triazolo-, Imidazo-, and Pyrrolopyrimidines and -pyridines. *J. Med. Chem.* **1999**, *42*, 833–848.
- (9) Dewar, M. J. S.; Thiel, W. J. Ground States of Molecules. 38. The MNDO Methodol. Approximations and Parameters. *J. Am. Chem. Soc.* **1997**, *99*, 4899–4907.
- (10) Dewar, M. J. S.; Zoebisch, E. F.; Healy, J. J. P.; Stewart, J. Development and Use of Quantum Mechanical Models. 76. AM1: a New General Purpose Quantum Mechanical Molecular Model. *J. Am. Chem. Soc.* **1985**, *107*, 3902–3909.
- (11) Kitson, D. H.; Avbelj, F.; Moul, J.; Nguyen, D. T.; Mertz, J. E.; Hadzi, D.; Hagler, A. T. Theoretical Study of the Regioselectivity of Successive 1,3-Butadiene Diels–Alder Cycloadditions to C60. *Proc. Natl. Acad. Sci. U.S.A.* **1993**, *90*, 8920–8924. The Biosym suite of programs is available from MSI, San Diego, CA.
- (12) Yakhontov, L. N.; Krasnokutskaya, D. M.; Akalaev, A. N.; Palant, I. N.; Vainshtein, Yu. I. *Khim. Geterotsikl. Soedin.* **1971**, *7* (6), 789–794.
- (13) Willette, R. E. Monoazindoles: The Pyrrolopyridines. *Adv. Heterocycl. Chem.* **1968**, *9*, 27–105.
- (14) Yakhontov, L. N.; Liberman, S. S.; Krasnokutskaya, D. M.; Uritskaya, M. Ya.; Azimov, V. A.; Sokolova, M. S.; Gerchikov, L. N. Azaindole Derivatives. XLVII. Synthesis and Pharmacological Study of 3-Aminoalkyl Derivatives of Azaindoles. *Khim.-Farm. Zh.* **1974**, *8* (11), 5–9.
- (15) Brodrick, A.; Wibberley, D. G. 1H-Pyrrolo-[2,3-b]-pyridines. Part III. A Novel Synthetic Route from 2-Aminopyrroles. *J. Chem. Soc., Perkins Trans. 1* **1975**, *19*, 1910–1913.
- (16) Pokorny, D.; Paudler, W. W. Naphthyridine Chemistry. XIV. The Meisenheimer Reaction of the I, X-Naphthyridines.
- (17) Hodge, C. N.; Aldrich, P.; Fernandez, C.; Chorvat, R.; Cheeseman, R.; Christos, T.; Arvanitis, A.; Scholfield, E.; Krenitsky, P.; et al. *Book of Abstracts*; 212th ACS National Meeting, Orlando, FL, Aug 25–29, 1996; American Chemical Society: Washington, DC; MEDI-094.
- (18) Aldrich, P. E.; Arvanitis, A. G.; Cheeseman, R. S.; Chorvat, R. J.; Christos, T. E.; Gilligan, P. J.; Grigoriadis, D. E.; Hodge, C. N.; Krenitsky, P. J.; Scholfield, E. L.; Tam, S. W.; Wasserman, Z. International Publication Number WO Patent 9510506.
- (19) Schulz, D. W.; Mansbach, R. S.; Sprouse, J.; et al. CP-154,526: A potent and selective nonpeptide antagonist of corticotrophin releasing factor receptors. *Proc. Natl. Acad. Sci. U.S.A.* **1996**, *93*, 10477–10482. Chen, Y. L. Pyrrolopyrimidines as CRF antagonists. WO 9413676-A1, 1994. Chen, Y. L. Pyrrolopyrimidines as CRF antagonists. WO 9413677-A1, 1994.
- (20) Oki, M. Applications of Dynamic NMR Spectroscopy to Organic Chemistry, *Methods Stereochem. Anal.* **1985**, *4*. Values of  $\Delta\nu$  obtained at the temperature closest to  $T_c$  were used in calculating  $\Delta G$ , although  $\Delta\nu$  did not vary significantly over the temperatures studied.
- (21) Finocchiaro, P.; Gust, D.; Mislow, K. Conformational Dynamics of Alkoxydiarylboranes. *J. Am. Chem. Soc.* **1973**, *95*, 7029–7036.
- (22) Cramer, R. D., III; Patterson, D. E.; Bunce, J. D. Recent advances in comparative molecular field analysis (CoMFA). *J. Am. Chem. Soc.* **1988**, *110* (18), 5959–67.
- (23) Chen, C.; Dagnino, R.; DeSouza, E. B.; Grigoriadis, D. E.; Huang, C. Q.; Kim, K.; Liu, Z.; Moran, T.; Webb, T. R.; Whitten, J. P.; Xie, Y. F.; McCarthy, J. R. Design and Synthesis of a Series of Non-Peptide High-Affinity Human Corticotropin-Releasing Factor Receptor Antagonists. *J. Med. Chem.* **1996**, *39*, 4358–4360.
- (24) Lam, P. Y.-S.; Ru, Y.; Jadhav, P. K.; Aldrich, P. E.; DeLuca, G. V.; Eyermann, C. J.; Chang, C. H.; Emmett, G.; Holler, E. R.; Daneker, W. F.; Li, L.; Confalone, P. N.; McHugh, R. J.; Han, Q.; Li, R.; Markwalder, J. A.; Seitz, S. P.; Sharpe, T. R.; Bachelier, L. T.; Rayner, M. R.; Klabe, R. M.; Shum, L.; Winslow, D. L.; Kornhauser, D. M.; Jackson, D. A.; Erickson-Viitanen, S.; Hodge, C. N. Cyclic HIV Protease Inhibitors: Synthesis, Conformational Analysis, P2/P2/Structure–Activity Relationships, and Molecular Recognition of Cyclic Ureas. *J. Med. Chem.* **1996**, *39*, 3514–3525.
- (25) Gewald, K. *Z. Chem.* **1961**, *1*, 349.

JM980223O